"NUMERICAL ANALYSIS OF MIXING PERFORMANCE IN A SPIRAL PASSIVE MICROMIXER"

MAJOR PROJECT-II

SUBMITTED IN PARTIAL FULFILLMENT OF THE REQUIREMENTS
FOR THE AWARD OF THE DEGREE OF

MASTER OF TECHNOLOGY
IN
THERMAL ENGINEERING
BY

SYED FARHAN JAVED, 2K17/THE/17

Under the supervision of

Dr. M. ZUNAID

ASSISTANT PROFESSOR

DEPARTMENT OF MECHANICAL ENGINEERING

DELHI TECHNOLOGICAL UNIVERSITY

(Formerly Delhi College of Engineering)

Bawana Road, Delhi-110042

JULY, 2020

CANDIDATE'S DECLARATION

I hereby certify that the work which is presented in the Major Project-II entitled "**Numerical Analysis of Mixing Performance in a Spiral Passive Micromixer**" in fulfillment of the requirement for the award of the Degree of Master of Technology in Thermal Engineering and submitted to the Department of Mechanical Engineering, Delhi Technological University, Delhi is an authentic record of my own, carried out during the period from January to June 2020, under the supervision of **Dr. M. Zunaid** (Assistant Professor), Delhi Technological University, Delhi.

The matter presented in this report has not been submitted by me for the award of any other degree of this or any other Institute/University. The work has been accepted in following Journal and conference ad its details are given below:

(I) Title of the Paper: Numerical Investigation inside Spiral Passive Micromixer using Nanofluid

Author names: Syed Farhan Javed[1], Mohammad Zunaid[2]

Name of Journal: (International Journal of Mechanical and Production Engineering Research and Development (IJMPERD) [Scopus Indexed Journal]

Have you registered for the publication: Yes

Status of paper: Accepted

Date of paper communication: 15/08/2020

Date of paper acceptance: 18/08/2020

Date of paper publication: NA

(II) Title of the Paper: Mathematical Analysis of a Spiral Passive Micromixer

Author names: Syed Farhan Javed[1], Mohammad Zunaid[1], Mubashshir Ahmad Ansari[2]

Name of Conference: Recent Advancements in Mechanical Engineering (RAME) [Scopus Index Proceedings Springer]

Conference Dates with Venue: 18-19 September 2020, Delhi Technological University, Delhi, India

Have you registered for the publication: Yes

Status of paper: Accepted

Date of paper communication: 10/06/2020

Date of paper acceptance: 20/07/2020

Date of paper publication: NA

Farhan

2K17/THE/17, SYED FARHAN JAVED

SUPERVISOR CERTIFICATE

To the best of my knowledge this work has not been submitted in part or full for any Degree or Diploma to this university or elsewhere. I, further certify that the publication and indexing information given by the student is correct.

Place: Delhi

Date: 18/08/2020

Dr. M. Zunaid

ASSISTANT PROFESSOR

DEPARTMENT OF MECHANICAL ENGINEERING

DELHI TECHNOLOGICAL UNIVERSITY

ACKNOWLEDGEMENT

It gives me immense pleasure to acknowledge all the people who have assisted me and guided me during my project work. I am grateful to my project supervisor **Dr. M. Zunaid** (Assistant Professor), Delhi Technological University, Delhi, for providing his constant support and guidance in all my efforts. Discussions with him always have been a source of great motivation to take up challenges and overcome them. It has been a real pleasure working with him. I am also thankful to all other faculty members of Delhi Technological University for sharing their knowledge and assist me whenever needed.

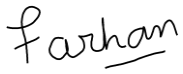

SYED FARHAN JAVED

(2K17/THE/17)

ABSTRACT

This research work possesses a mathematical analysis and contrasting of mixing characteristic and flow behavior inside microchannels with different geometries: Simple T shape and Spiral/Helical shape (with and without nanofluid). Micromixing has become very popular and useful contemporarily. The flow analysis is carried out using Navier-Stokes equations and mixing performance of two fluids, namely; water and dye is numerically calculated. The dye is infused with 1% Al_2O_3 in the case of a spiral T shape micromixer with nanofluid. The boundary conditions are specified in terms of suitable velocity at the two inlets and the pressure is set as zero static at the micromixer outlet. The mixing performance is calculated concerning mixing index or efficiency of mixing. The spiral T shape mixer creates the vortices and makes the swirling flows even at low Reynolds numbers in comparison to a basic T shape mixer. The circular cross-section at the beginning of mixing spiral microchannel enhances the contact surface area of the fluid by widening the flow. The proposed spiral microchannel is found to be efficient in mixing fluids at a vast range of Reynolds numbers. The three micromixers are observed, analyzed and their mixing index is finally observed at different Reynolds number, namely 5, 45, 165, and 350. This suggested mixer is easy to design and fabricate and provides a wide control for the mixing index based on Reynolds number. The results possess that the mixing in a spiral microchannel is very subtle to the input variables, exhibiting different characteristics at different Reynolds numbers. This research is helpful in the biomedical and biochemical sciences, and their applications in fields such as cell storage, screening, cancer detection techniques, DNA analysis, dynamic cell separators, etc.

CONTENTS

LIST OF FIGURES

LIST OF TABLES

ABBREVIATIONS

Symbol	Description
TMC_x	Circular topological micromixers
TPZ	Zigzag topological structure
$TMRF_x$	Topological micromixers with reversed flow
TZM	Trapezoidal zigzag micromixer
CLDH	Cross-linked dual helical
SAR	Split and recombine micromixer
Re	Reynolds number of the fluid flow
ρ	Density of the fluid, kg/m^3
L	Characteristic length of the mixing channel, µm
μ	Dynamic viscosity, $N\text{-}s/m^2$
V	Relative velocity, m/s
D_h	Hydraulic diameter of the mixing channel, µm
Q	Volumetric flow rate, m^3/s
ν	Kinematic viscosity, m^2/s
A_c	Cross-sectional area, μm^2

P_m	Perimeter of mixing channel, μm
ρ_f	Density of the base fluid, kg/m^3
ρ_{nf}	Density of the nanofluid, kg/m^3
ρ_p	Density of the solid particles, kg/m^3
η	Mixing Index
c	Concentration at a specific point
$\bar{c}^0$	Unmixed scale concentration
$\bar{c}^*$	Perfect mixed scale concentration
N	Number of sample points on a selected cross-section

CHAPTER 1

INTRODUCTION

1.1 Introduction

This chapter will briefly describe the introduction of micromixers and also about nanofluid. In this research study, the problem statements are related to biomedical, chemical analysis. The two fluid phases should be well mixed to make the best efficient solution. Along with this, the particular problem and procedure of this research are also mentioned for a better insight into this micromixing field. Then the significance of this study, research objectives, viable scopes, and expected results will be shown in detail in this investigation.

1.2 Background Study

At macroscale level, generation of turbulence in the flow assists in mixing, but at low Reynolds numbers, the micromixing in devices depends mainly on diffusion on account of laminar flow regimes. Micromixing is a phenomenon that incorporates the use of the advection and diffusion process. Micromixing takes place inside the channels known as microchannel. The micromixing devices are broadly used in different fields of scientific technologies as microscale heat exchangers, microreactors, micromixers, etc. Most micromixing devices used in biology and chemistry field require rapid and optimum mixing of fluids.

Micromixers are categorized and differentiated as active and passive micromixers. The passive micromixers contain no moving mechanism or external part. The delivery of the fluids is done by micro-valves or micro-pumps to the mixing channel but they are considered as external parts to this mixer. The active micromixers contain moving mechanisms or part that adjusts or governs the pressure gradients in the mixing geometry. Due to the dissimilarity in the mixing mechanisms, the

active mixer is also referred to as dynamic whereas passive mixer is referred to as static. Due to the fact that passive micromixers are simple in structural geometry and easy to control, so, they are very much suitable for micromixing fields.

To create rapid mixing in a flow, generation of turbulence and churning makes it possible by partitioning the fluid in different sections, where the contact surface area gets increased and the mixing length gets reduced. But, as we know that the Reynolds number is very less in micromixing devices of the order of 1 or even less, very much below the transitional Reynolds number, hence, turbulent generation is not possible. Every micromixer operates in the laminar region of flow and depends completely on the diffusion process. So, the factors required for better results are compact channel area, rapid mixing duration, and ability to integrate with a system.

The passive micromixing process depends completely on molecular diffusion, as well as on disorderly advection. The mixing in passive micromixers can be classified further as parallel lamination, serial lamination, injection, chaotic advection and droplet mixing based on the different settings of the mixing fluid phases while active micromixers use external sources for enhancing the mixing phenomenon. The mixing in active micromixers can be further classified on the basis of types of interference created by an external source and medium as temperature-induced (thermal), pressure-driven, electro-hydrodynamic, di-electrophoretic, electro-kinetic, magneto-hydrodynamic, and acoustic concepts. Due to additional parts and supplying power externally for the generation of turbulent regimes, the fabrication of active micromixers is usually sophisticated. Therefore, the unification of active mixers in a micromixing module is both time taking and costly. The main benefit of operating passive micromixers is the absence of external sources or actuators. On the other hand, passive geometries are simple, robust, stable in working, convenient to control and integrate [1-3]. Types of micromixers are shown below (Fig.1.1).

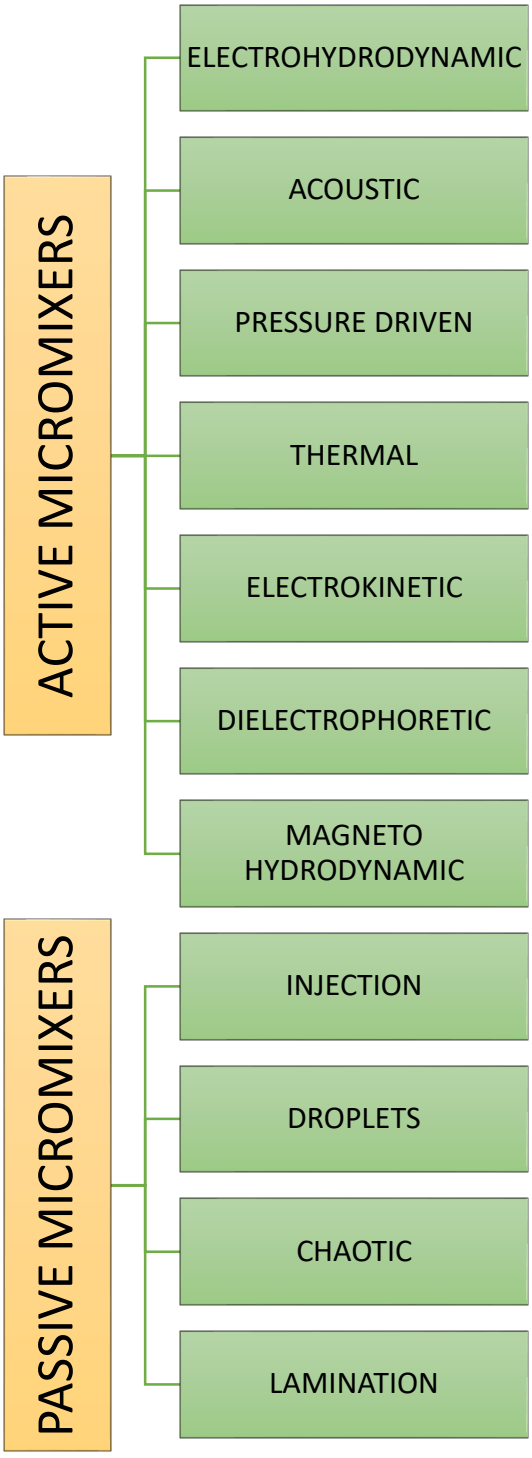

Fig.1.1 Different types of micromixers

1.3 Nanofluids

The nanofluids came into the picture about two decades ago in a laboratory in the USA. The use of nanofluid in recent years in heat transfer applications has raised its importance due to its viable dominance that includes great stability, high heat stability, and also enhanced drop in pressure. In nanofluids, usually, water acts as the base fluid with nanoscale metallic /non-metallic particulates. The properties that define a nanofluid are density, viscosity, thermal conductivity, specific heat, and stability. These properties have a very important role in the preparation of nanofluids. In this numerical investigation, only 1% concentration of Al_2O_3 is used as the nanofluid particle with pure water as its base.

1.4 Problem Statement

In general, higher efficiency is obtained in active micromixers. But, the need to incorporate external mechanisms such as the actuators for externally providing power into the micromixing device, and the sophisticated, costly process of fabrication, restricts the use of these devices practically. Also, the ultrasonic waves and high-temperature gradients during active mixing phenomena can deteriorate fluids biologically. Hence, when encompassing micromixing practically in biological and chemical applications, these active micromixers are not the right option to choose. The passive micromixing devices depend completely on the pressure of the fluid and different channel designs are used to enforce the flow in a manner that shortens the diffusion mixing length and increases the interfacial cross-section. The passive micromixers were the foremost reported micromixers. They generally involve low cost and are more easily fabricated than active micromixers. They can also be conveniently organized for specific problems. The reduction in time for mixing fluids is basically reduced by segregating the fluid flow using parallel or serial lamination, infusing gas bubbles generally slug or droplets of liquid into the flow, increasing chaotic advection by incorporating grooves or ribs designed on the walls of the channel. The mixing in macroscale devices can be characterized by eddy diffusion, molecular diffusion, chaotic advection, and Taylor dispersion. The Eddy diffusion requires a turbulent flow as it requires the transportation of species. As we all know that viscous effects are dominant in the case of micromixing, due to which turbulence cannot be generated. Hence, the eddy diffusion process is irrelevant in the case of micromixers. Therefore, only molecular diffusion, Taylor dispersion

and chaotic advection are the major phenomena for transportation in micromixers. The molecular diffusion takes place by the molecules random motion. The coefficient of molecular diffusion characterizes this phenomenon of transportation. The phenomenon that takes place by the motion of the fluid is advection.

The chaotic distribution can be led by simple Eulerian velocity of the mixed species and also by a suitable laminar flow. Hence, in micromixers, the chaotic advection is most suitable for the laminar flow. The advection caused by the velocity difference in flow is Taylor dispersion whereas the axial dispersion is caused because of advection and different velocity layers inter-diffusion. The micromixing based on Taylor dispersion is increased two to three folds as compared to micromixing relying only on pure molecular diffusion.

1.5 Significant Study

In this research, the latest geometry of a passive micromixer is fabricated and analyzed. It assists researchers in the medical field in making the comparison of different available designs for minimal mixing time and also to understand the conceptual details. These sorts of designs can also be implemented in the lab on chips and more efficient and faster results can be obtained. It will assist in biomedical fields like the doctor can suggest suitable treatment to a patient based on the investigation results of micromixer. It also helps in the detection of cancer-causing cells.

1.6 Objectives

The following points are the basic aim of the research:

- To fabricate a new geometry of the passive micromixer.
- To observe the mixing characteristics of fluids and its performances through mass fraction contours and calculation of mixing index amongst the stated micromixers.
- To carry out a relative comparison of spiral T shaped passive micromixer (with and without nanofluid) of the same characteristic geometrical dimensions with simple T micromixer.

1.7 Scope

The passive micromixers are available in different designs e.g. basic shape, serial-parallel lamination micromixer, chaotic advection micromixer, injection micromixer, sequential lamination micromixer, and droplet micromixer. A diversified analysis needs to be carried out for this project report. To compare the different micromixer's designs, it takes time and also resources. The designing and fabrication of micromixers is an entirely different field, as the available macroscale designs cannot be directly synchronized for microscale utilization. The main challenge faced in the miniaturization of the devices is to compensate volume effects by surface effects. The concept of actuation depending on volume forces that mesh with macroscale devices may not be compatible with microscale devices.

Another challenge apart from surface phenomena is the laminar flow regime for fabricating micromixers. In micromixers, the velocity of flow cannot be set too high for different applications. The compact geometry of micromixers leads to heavy shearing stresses, even at low flow velocity. This induced shear may lead to cell damage and other bio-particles. Chaotic advection leads to mixing improvement in the flow of fluid even at lesser Re. Generally, molecular diffusion based passive micromixers have the same direction of chaotic advection as of main flow. Therefore, the transversal movement of species depends completely on molecular diffusion. The secondary transversal movement can be caused by three-dimensional advection and it also improves mixing significantly. The basic micromixer design viable for the advection generation is the channel shape modification for elongating, overlapping, and separation of this laminar flow.

In this research, a newly designed passive micromixer is fabricated and analyzed. The modification of the internal shape and structure of the micromixing channel can enhance the contact surface area and thereby enhance the performance of mixing. The helical nature of the micromixer enforces the two liquids to fuse into each other within an optimum length. The further use of nanofluid as one of the fluid at the inlet of passive micromixer enhances the mixing efficiency and opens the gateways for further study in this field.

CHAPTER 2

LITERATURE REVIEW

2.1 Overview

A lot of research investigations have already been done in the field of micromixing. In the section mentioned below, recent research work related to passive micromixing is discussed. Section 2.2 introduces us to the proposed research findings regarding passive micromixers design, fabrication and the results obtained.

2.2 Recent Papers Regarding Micromixing

Chen Y et al. [4] designed a passive micromixer that uses the topology optimization method. In this research, original structures are taken as circular and compared with a series of topological micromixers (TMC_x), circular structures. The mixing efficiency is appreciably improved by using the topology optimization method. At Re = 10, for the Circular micromixer, efficiency is only 91.9% whereas, for the topological micromixers, the mixing efficiency obtained at the outlet is 95.9%.

Vijayanandh V et al. [5] designed a passive micromixer in which simulation is done with ridges for increment in efficiency. In this research work, channels of micromixer geometries are designed and for different fluids, their flowing patterns are observed to establish optimal mixing. It is found that the appreciable increment in mixing efficiency is in the case of micromixers with ridges.

Shah I et al. [6] implemented a new method known as the Taguchi method for the suitable mixing of active and passive micromixers. In this investigation, three novel mixing designs are discussed: active micromixer, passive micromixer and a combination of active and passive mixer. The further increment of the mixing index of the basic active micromixer is done by using the Taguchi method. This method is implemented and varied against criteria such as velocity, voltage, and frequency. The result of this investigation shows that basic active micro-mixer at t=0.2 s achieved 99.6% mixing efficiency along with velocity of 0.05 mm/s, voltage of 0.5 V, and frequency of 10 Hz.

Lobasov S et al. [7] studied the water and ethanol fluid mixing inside a simple T shape micromixer. The variation of the fluids mixing index and the drop in pressure against Reynolds number is investigated, and mixing flow regimes are also analyzed. It is observed that the ethanol when mixed with water results in a greater drop in pressure compared to the case of the water mixing with water.

Hossain S et al. [8] studied a passive micromixer, serpentine two-layered crossing channels for low Re mixing. The numerical investigation is done using 3-D Navier-Stokes theorems. The convection–diffusion module is used for the concentration of species in a range of Reynolds number varying from 0.2 to 120. Two fluids, namely water and water-dye mixture are used. The micromixer exhibited mixing greater than 95% throughout the investigated values of Reynolds number. At the Reynolds number less than 10, 99% mixing is achieved.

Chen X et al. [9] designed an optimal algorithm for a novel passive micromixer in a zigzag microchannel. The topology optimization method when applied to this zigzag structure, a new mixer, knowns as TPZ, is introduced. This TPZ delivers great performance at a very wide range of Re less than 0.5 or greater than 5. The mixing indices observed in this range are greater than 93%. Even for a range of Re, between 0.5 and 5, around 90% efficiency is still achieved.

Chen X et al. [10] fabricated the passive micromixers depending on the topology optimization technique. The series of $TMRF_x$ i.e. topological micromixers with reversed flow namely, $TMRF_{0.25}$, $TMRF_{0.5}$, $TMRF_{0.75}$, shows better results than the square wave micromixer at different Reynolds numbers, but drop in pressures of $TMRF_x$ are somewhat higher. For a vast range of Re i.e. less than 0.1 or greater than 10, the mixing efficiency in $TMRF_{0.75}$ is higher than 95% and possesses better performance. Even for Re ranging from 0.1 to 10, the $TMRF_{0.75}$ possessed an efficiency of greater than 85 %.

Viktorov V et al. [11] studied the fluid mixing numerically at different inlet flow-rate ratios in chain and tear-drop micromixers in comparison to a new h-c passive micromixer. The mixing characteristic is analyzed numerically at Re ranging up to100, with the inlet flow-rate ratio variation. The H-C micromixer shows a mixing efficiency of around 90% and better than the Tear-drop and Chain micromixers. It also depicts independency on Reynolds numbers. Also, it has a negligible dependency on the inlet flow-rate ratio of the H-C mixer.

Li X et al. [12] designed a three-dimensional overbridge-shape for rapid mixing over a vast range of Re. By numerical analysis, around 90% efficiency has been achieved for Re ranging from 0.01 to 200, and also experimentally, it is observed the same mixing efficiency is obtained but within a Re range from 0.01 to 50. Even for mixing of two fluids at the two inlets with different rates of flow varying from a ratio of 1:9 to 9:1, around more than 90% efficiency is also achieved.

The H et al. [13] studied a passive micromixer with trapezoidal-zigzag channels for performance analysis. This research investigates about mixing characteristics of the TZM at different Re, namely 0.5, 5 and 50. The TZM with six mixing units, a narrow height of 100 μm, having a width ratio of 0.5, the trapezoidal slope angle of 75° possesses the topmost mixing efficiency. The TZM possesses a mixing efficiency of more than 85% for a range of Re from 0.1 to 80. Moreover, for Re less than 0.9 and Re more than 20, this TZM micromixer shows a mixing efficiency of more than 90%.

Yang A et al. [14] designed a new micromixer that uses 3-D tesla structures for biotech- related applications. The theoretical and practical results of this micromixer show great mixing characteristics for Re varying from 0.1 - 100 (0.015–15L/s). It depicts the successful implementation of this mixer to the immunofluorescence analysis of the EGF receptor. It detects antigens that cause lung cancer.

Andreussia T et al. [15] analyzed the flow regimes inside T-shape micromixers. The various values of the aspect ratio i.e. width to height ratio of the inlet channels, ‘i’ are taken into account and specifically at ‘i’ equals 0.75, 1 and 2. The performance is almost the same at aspect ratio i= 0.75 and 1. The case is entirely different for i= 2. For the Re equals 220–240, the vorticity characteristics turns unstable and also time-periodic but somewhat sticks to its central point symmetry.

Rasouli M et al. [16] investigated T-shape micromixers with obstacles for low Re. It is evident from this research that a T-shape micromixer with obstacles and with grooves enhances the efficiency of mixing by 37.2% and 43.8%, respectively from the basic design. The grooved T-shape micromixer achieves 88% optimal mixing efficiency and also reduces the mixing length, making it suitable for Lab on Chip applications.

Liu K et al. [17] fabricated a new cross-linked dual helical micromixer and analyzed it for fast mixing at lesser Re. The numerical simulations are performed to analyze mixing inside the CLDH micromixer. In a very short length, the CLDH mixer possesses an excellent mixing potential for a vast Re range. The mixing index of around 0.99 could be obtained in four cycles (almost 320 μm length) for Re ranging from 0.003 to 30.

The L et al. [18] implemented the mechanisms for multi-mixing in micromixer for enhanced mixing efficiency at low Re. This stated micromixer could achieve mixing efficiency of greater than 80% for a vast range of Re from 0.5 to 100. In specific, for Re greater than 30, mixing efficiency depends negligibly on Reynolds number. At Re equals 30, this stated micromixer shows 85% mixing efficiency with an optimal drop in pressure, $\Delta P = 12{,}600$Pa.

The L et al. [19] investigated the trapezoidal blades micromixer for enhanced mixing performance at low Re. In this research, the simulation results depict that the micromixer can attain much greater mixing efficiency without Re dependence whilst varying from 0.5 to 60. Moreover, at very low Re, the mixing efficiency of this micromixer is 220-240% greater than the pure rhombic mixer or rhombic mixer with branch channels.

Tran-Minh N et al. [20] optimally analyzed passive micromixer with elliptical micropillars for the fusion of human blood. In this research, micromixer with elliptical micropillars possesses enhanced mixing efficiency of about more than 80% at Re less than 1. In specific, this sort of micromixers may be optimal for a rapid, optimal and convenient collection and better mixing of fluids. This can be viable for sample preparation of entire blood or biological fluids used in diagnostic applications.

Afzal A et al. [21] considered the periodic variation of the velocity profile in the multi-objective optimization of a passive micromixer. In this research, the steady Navier–Stokes equations are used at the specific Re = 0.91. Considering design parameters, the mixing performance increases with higher geometrical aspect ratios a/H and lower of b/g and h/H values.

He X et al. [22] studied a passive micromixer with a logarithmic spiral channel and its mixing performance is analyzed. The micromixer's mixing performance is observed at Reynolds numbers varying from 0.2 to 100. The results possess that the index of mixing at the outlet of the micromixer decreases with increasing Re, up till it reaches 5.0. Beyond Re = 5, the mixing index improves and thereby delivers better performance.

Hossain S et al. [23] analyzed a passive micromixer that incorporates unbalanced three-split sub-channels that are rhombic. This proposed micromixer's performance and drop in pressure are calculated and collated to that of two-split passive micromixer for Re ranging from 0.1 to 120. The obtained results suggest that this proposed micromixer is optimal for Re ranging from 30 to 80.

Li J et al. [24] investigated a planar SAR (split and recombine) micromixer with dislocation sub-channels numerically and experimentally. The numerical simulations and experiments are carried out to analyze the influence of input constraints with flowing characteristics on mixing performance by varying Re from 1 to 100. The increment in width ratio embedded by the dislocation structures leads to improved mixing efficiency, but also leads to a larger drop in pressure.

Wang L et al. [25] studied a passive micromixer for performance enhancement that contains triangle restrictions or baffles. At Re = 1.0, within a distance of 6.4mm, the mixing efficiency is found to be 85.5% and is 2.48 times better than a basic Y-shape micromixer. At the same stated distance, at Re = 100 and Re = 500, this micromixer shows 4.75 times and 8.32 times respectively better mixing efficiency than a basic Y-shape micromixer.

Alam A et al. [26] studied a planar micromixer that has curved microchannels with circular obstructions. The water and ethanol are taken as the working fluids. The governing Navier-Stokes theorem along with diffusion equation is used for Re ranging from 0.1 to 60. This micromixer shows the best mixing index at Re = 1 and Re > 15 with an efficiency of 88% while the lowest mixing index is found to be 72% at Re = 5.

Wu C et al. [27] proposed a micromixer with zigzag channels and semi-elliptical walls in which vortices generated multi-directionally. The mixing index of this proposed micromixer with a greater aspect ratio denoting maximum width to minimum width is found to be better than the basic twisted micromixer with the same cross-section throughout for a high flow rate along with small curvature.

Alam A et al. [28] investigated a planar micromixer that has circular chambers and constriction passages. This micromixer is found to achieve a mixing efficiency of 88% at Re equals 0.1 with 8 mixing circular chambers but the mixing index of this micromixer is less than that of the other conventional micromixers for $Re > 10$. Hence, this micromixer is viable and optimal for use for $Re < 10$.

Yang J et al. [29] designed and fabricated a three-dimensional micromixer of spiral shape. Dean vortices can be suitably generated for disturbing the laminar flow of fluid efficiently. Around 90% of mixing efficiency has been attained by adjusting the rate of flow and the geometry of the channel. The further simulation investigation exhibits that by attaching one more semicircle for the spiral shape channels, about 99% mixing efficiency could be attained.

Feng X et al. [30] fabricated an optimal SAR (split and recombine) micromixer with a self-rotating contact surface for a vast range of Re. This micromixer is fabricated by multiple-layer soft lithography. The mixing efficiency for this proposed micromixer is found to vary from 91.8% to 87.7% for Re values ranging from 0.3 to 60, whereas for the corresponding micromixer it varies from 89.4% to 72.9%.

Ansari M et al. [31] fabricated a T-mixer with non-aligned inputs for generating vortex. In this research, the simulation results of this proposed vortex T-mixer are calculated and then compared with that of a simple T-shape micromixer. This mixing geometry generates the vortical flows that support mixing even at low Re, thus possesses better performance in comparison to a simple T-shape micromixer.

Scherr T et al. [32] fabricated a planar micromixer that uses logarithmic spirals. At the beginning as the Re increases, the mixing efficiency possesses a drop, and this nature continued up till a Re 15 and 53% efficiency is observed. After that, mixing efficiency starts to increase and reaches the mixing efficiency of about 86% at Re equals 67. Though, another sort of micromixer SeLMA possesses higher efficiency of about 10–15% than both the Archimedes and Meandering-S mixer designs for Re values greater than 15.

Afzal A et al. [33] designed a passive SAR (split and recombine) micromixer with convergent–divergent sidewalls. The proposed micromixer is analyzed for Re ranging from 10 to 70. The micromixer that has a higher amplitude wall of the channel shows better mixing performance due to induced secondary motion. At an amplitude of 0.25 mm and Re equals 70, the fabrication of the sinusoidal channel wall with eight cycles possesses a mixing efficiency of about 90 percent and a pressure drop of 12 kPa. Moreover, by enhancing the aspect ratio of the cross-section of the channel, the mixing efficiency is enhanced and the loss of pressure is reduced.

Sheu T.S et al. [34] studied a passive micromixer, SAR (split and recombine) with tapered curved microchannel and the comparison is done between four different designs of a curved microchannel. The mixing efficiency of the tapered channel, staggered curved-channel mixer is found to be 20% greater than the other curved micromixers but the drop in pressure of this staggered curved-channel mixer is found to be around 50% greater than the other two staggered curved-channel mixers. It is evident that it is suitable for Re more than 5. At the Re = 50, for the same mixing performance, the channel length of flow has been reduced five folds in comparison to the case where Re = 1.

Hossain S et al. [35] fabricated and analyzed a passive micromixer using a modified Tesla structure. The aspect ratio i.e. the ratio of the diffuser gap to the channel width and the ratio of the curved gap to the channel width is varied for mixing performance and drop in pressure analysis from Re varying from 0.05 to 40. The effective results depict that the geometric parameter variation plays a significant role in mixing characteristics and for a drop in pressure.

Ansari M et al. [36] designed the novel micromixer with unbalanced splits and considering collisions of fluid. In this research, the investigation at Re varying from 10 to 80 is studied numerically and experimentally. This micromixer's performance is analyzed for various ratios of the widths of the two split sub-channels. The highest mixing performance is observed in the case of sub-channels where the major sub-channel width is two times as the minor sub-channel at Re = 40. In the case of uniform width, the lowest mixing performance is observed due to balanced collisions.

Dreger S et al. [37] studied laminar transient flow characteristics and mixing in T-shape micromixers. Firstly, in Dean-flow, symmetrical vortices are generated for Re > 10. Thereafter, fluid shifts to the opposite side at Re > 140 and generates a double vortex, which improves mixing. Beyond Re = 240, a sort of wake is generated and it becomes unsteady and in between Re 240 to 500, there is periodical wake flow with a Strouhal number approx. 0.23. The mixing index is also found to decrease for Re > 500. By further increasing the Re to 1000, the normalization of the pulsations is perturbed due to frequencies, resulting in a chaotic nature of the flow.

Hossain S et al. [38] observed and analyzed the mixing performance for three passive micromixers. The analysis in the micromixers is done by using two fluids, namely water and ethanol. Numerically, the square wave microchannel possesses the best optimal mixing efficiency, whereas the curved and the zig-zag microchannels for most of the Reynolds number possess nearly the same mixing characteristics. The smallest drop in pressure is observed in curved micromixer, whereas the zig-zag and square wave channels show the same drop in pressure.

Ansari M et al. [39] analyzed a three-dimensional serpentine microchannel using two fluids. Two geometrical aspect ratios, i) height to width of channel ii) straight channel length in an "L-shaped" unit to the width of the channel is observed for various Re. The serpentine microchannel with "L-shaped" repeating units is found to be more efficient in mixing the fluids at specified Re = 1, 10, 35, and 70. Both the mixing index and vertical circulation is enhanced through most of the mixing length for Reynolds number varying from 1 to 70.

Tofteberg T et al. [40] designed a novel passive micromixer by lamination in a planar channel system. In this module, the cross-section of flow is rotated by 90 degrees in each channel to be followed by several channel split. The interfacial area is doubled by recombination between the two given fluids. Until desired mixing performance, this is continuously repeated. The results of this micromixer are verified with prototypes both experimentally and numerically.

Asgar A et al. [41] studied a passive planar micromixer for mixing at low Re using obstructions. A planar passive micromixer is designed, fabricated and simulation results are obtained for low Reynolds number micromixing. Simulation results as well as experimental results show its capability of mixing. It gives optimal results for $0.01 < Re < 100$ numerically, while gives better results for $0.02 < Re < 10$ experimentally. This proposed micromixer also shows a small pressure drop.

Wong S et al. [42] investigated the T-shape micromixer is investigated as a fast mixing micromixer. The micro T-mixers are designed and investigated to check whether they are optimal or not as a rapid mixing micromixer. A blue-colored dye and a colorless liquid are used for mixing analysis. Then di-chloroacetyl phenol red is used for further investigation and chemical reaction. It was found that at $400 < Re < 500$, it can be treated as a rapid micromixer.

CHAPTER 3

LAWS FOR MICROMIXING

3.1 Flow of Fluid and Reynolds Number

The flow of the fluids is usually classified into two zones, i.e. laminar and turbulent. The laminar fluid flow is identified by smooth and continuous movement whereas turbulent flow is identified by vortices and zigzag motion. The characterization of the fluid, whether it is laminar or turbulent is distinguished by Reynolds Number generally written as Re. It is a dimensionless number that was coined to determine the relative value of inertia forces in comparison to viscous forces in the flow. The Reynold Number (Re) is shown below in Equation (3.1).

$$Re = \rho * V * L / \mu = V * L / \nu \tag{3.1}$$

In the above-stated equation, ρ is the density of fluid used, μ is the dynamic viscosity, ν is the kinematic viscosity, V is the relative velocity and L is the characteristic length along measured the flow.

The flow of the fluid with Re > 1 tends to be turbulent whereas for Re < 1, the flow of fluid is laminar. In micromixing flowing regimes, the measured scale values are too small, so the fluid flow is considered laminar. Micromixing channels (generally closed pipe) adopt a number of different geometries that are not circular. So, length in the Re equation given above is usually substituted by the hydraulic diameter (D_h) as given in Equation (3.2).

$$Re = \rho * V * D_h / \mu = Q * D_h / (\nu * A_c) \tag{3.2}$$

The hydraulic diameter D_h can be calculated according to the formula given below in Equation (3.3).

$$D_h = 4A_c / P_m \tag{3.3}$$

In equations stated above, Q is the volumetric flow rate, A_c is the area of cross-section of mixing channel and P_m is the perimeter of mixing channel given in Equation (3.2) and Equation (3.3). Like the hydraulic diameter for a square channel of side 'a' is given below (Fig 3.1).

'a'

Fig. 3.1 Hydraulic diameter, D_h = 'a' for the square shape flow channel

At low Reynolds number, the flow is laminar and the mass transport occurs only in direction of fluid flow, hence the mixing can take place only through diffusion and advection. The movement of viscid fluid flow is administered by the Navier-Stokes equation, which takes into account volumetric flow rate, Q (m^3/s) as stated in Equation (3.4).

$$Q=VA_c \tag{3.4}$$

Here, V is the relative velocity of the flow.

3.2 Properties of the Fluids Used

The thermodynamic fluid properties include pressure, temperature, and density, whereas the mechanical properties include viscosity, surface tension, and thermal conductivity. In the micromixing phenomenon, for the movement of fluids in micromixing channels, static pressure is often used as the triggering force, whereas temperature, governs the fluid's internal energy. Likewise, the density is dependent on both temperature and pressure. The fluid's mechanical property, viscosity is a vital property as it resists the motion due to shear stress applied on a fluid.

Any sort of temperature gradient in micromixing systems results in heat transfer. Another property i.e. thermal conductivity depends on the temperature and pressure.

3.2.1 Density

The density, ρ of the fluid is defined as the mass of fluid per unit volume occupied (kg/m^3). Even in the presence of pressure, it is considered as constant due to the incompressible nature of liquids. Specific weight, γ depends upon the density and is defined as the weight of fluid per unit volume of the given fluid as given in Equation (3.5).

$$\gamma = \rho g \tag{3.5}$$

In the above equation, g is the gravity constant ($g=9.8m/s^2$). The unit obtained of specific weight is N/m^3. Assuming the density as constant and the fluid to be stationary, we can state hydrostatic pressure, P as given in Equation (3.6).

$$P = \rho g h \tag{3.6}$$

Where h is the height/altitude measured in the gravity direction.

3.2.2 Viscosity

Viscosity is the resisting measure offered by the fluid due to either shear or tensile stress applied. The value of viscosity is directly proportional to the offered resistance by the fluid. Generally, if the viscosity of a liquid is less than water, then it is termed as a mobile liquid whereas, in the opposite scenarios, it is termed as a viscous liquid. The physical characteristics related to viscosity are defined below:

a) Molecular layers possess a velocity gradient in any sort of flow.

b) The fluid's viscosity comes in picture when due to any applied force shear stress opposes it. We are here dealing with the kinematic viscosity, ν (m^2/s). It relates the dynamic viscosity with the density as given in Equation (3.7).

$$\nu = \mu/\rho \tag{3.7}$$

Where the absolute viscosity, μ (Ns/m^2, Pa.s) is the resisting potential of fluid offered to its motion. Newtonian fluids are termed as such that they are independent of the viscosity of the velocity gradient. It should be known that viscosity is dependent upon temperature and the fluid possesses less viscosity if the temperature is increased. In this research, we have assumed that there is no temperature gradient during the analysis of micromixing devices.

3.3 The Continuum Model

The assumption of continuum generally holds true for micromixing models. The fluid properties are well defined in space and can be considered as a continuum, and taking the density at a point as sufficient property.

3.3.1 Navier-Stokes equation

Since viscosity is not varying with temperature, the fluid flow is treated as incompressible, hence the energy can be eliminated. The equation governing the fluid flow analysis is the Navier-Stokes equation {(3.8) and (3.9)} altogether for incompressible flow and also non-turbulent fluid flows.

Continuity equation

$$\nabla . \mathbf{V} = 0 \tag{3.8}$$

Momentum equation

$$\rho \frac{D\mathbf{V}}{Dt} = -\nabla P + \rho \mathbf{g} + \mu \nabla^2 \mathbf{V} \tag{3.9}$$

Where,

$\rho \frac{D\mathbf{V}}{Dt} = \rho \left[\frac{\partial \mathbf{V}}{\partial t} + (\mathbf{V} . \nabla)\mathbf{V} \right]$, known as Total Derivative,

$\frac{\partial \mathbf{V}}{\partial t}$ = Change of velocity with time and $(\mathbf{V} . \nabla)\mathbf{V}$ = convective term,

$-\nabla P =$ Pressure gradient,

$\rho \mathbf{g} =$ Body force,

$\mu \nabla^2 \mathbf{V} =$ Diffusion term

The terms stated in above equation in the bold are vector quantities.

CHAPTER 4

METHODOLOGY (I)
SPIRAL T MIXER (WITHOUT NANOFLUID)

4.1 Description of the Problem

In order to increase the micromixing efficiency of two fluids with different thermo-physical properties, many types of researches have already been carried out. There are many active and passive micromixers of different geometries and different innovative structural developments. In this paper, we will first fabricate the geometry and then observe and numerically simulate the mixing efficiency of the two fluids, namely; water and dye (same thermo-physical properties as of water) inside the **Spiral T shape passive micromixer**. Then, we will compare the obtained results with that of the simple T shape passive micromixer of the same volumetric size. The spiral T shape micromixer is further investigated by adding nanofluid (1% Al_2O_3) and then the results of this are also compared with other stated passive micromixers.

4.2 Geometrical Construction

The geometries of both the simple and spiral T shape micromixers are fabricated in commercial CAD software Solid Works. In the spiral shape micromixer, the spiral channel is attached separately to the rectangular cross-section bar using assembly operations in Solid works. The assembly is then converted into a single body using suitable commands. Then the geometry has been imported to commercial ANSYS workbench software in suitable supported formats. The

geometry is then opened and edited using the design modeler setup for geometry. Then it is being subjected to mesh operations for further analysis of the micromixer.

4.3 Geometrical Modification

In order to have the same mass flow rate, we have to assign the same inflow area of the inlets. The mixing channel is given the shape of the spiral with almost two revolutions. The diameter of the mixing spiral channel is made as such to accommodate the two fluids gushing towards the channel. The mixing channel is appropriately adjusted to have the same mixing length. In order to attach the spiral to the inlet fluid channel, there are adjustments needed to incorporate the same mass flow rate as the one we are validating with. Therefore, the inlet faces are of rectangular cross-section and the outlet is circular cross-section i.e. at the end of the spiral mixing channel. The specifications of the simple T shape and Spiral T shape micromixers are given below in Table 4.1.

Table 4.1 Geometrical dimensions of micromixers

Type	Simple T shape dimensions (μm)	Spiral T shape dimensions (μm)
Inlet cross section	100*100	159.5769*62.6657
Non mixing channel length	800	800
Mixing channel diameter(d_h)	133.3333	159.5769
Mixing channel length	3000	~3000
Spiral Diameter (D)	-	400
Spiral Pitch (p)	-	2000
Spiral Turns (n)	-	~1.25

The fabricated spiral/helical shape micromixer obtained in commercial Solid works software is given below (Fig.4.1).

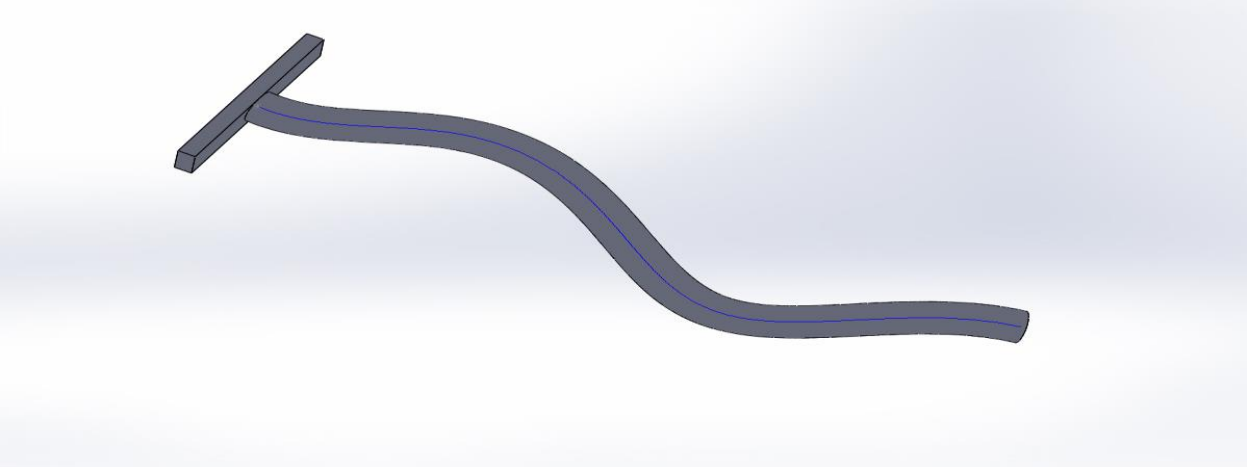

Fig.4.1 Spiral T shape passive micromixer

4.4 Meshing

Meshing is one of the basic and important parts of the simulation module. In this section, complex geometrical body contours are split up into simple elements which are then approximated discretely for larger domains. The meshing model affects the accuracy, convergence and time of the simulation. The ANSYS software imbibes basic purpose meshing and also great performance, automatic intelligence meshing program that generates the most suitable mesh for precise monitoring and effective solutions. It varies from convenient and automatically generated mesh to sophisticated custom meshing. Before generating this mesh, the critical zones need to be rectified like the zones where the curvature is changing, etc. After that, the meshing setup is set as adaptive and all the meshing nodes and elements are generated by ANSYS solver. The mesh obtained after imbibing all the details is shown below (Fig.4.2).

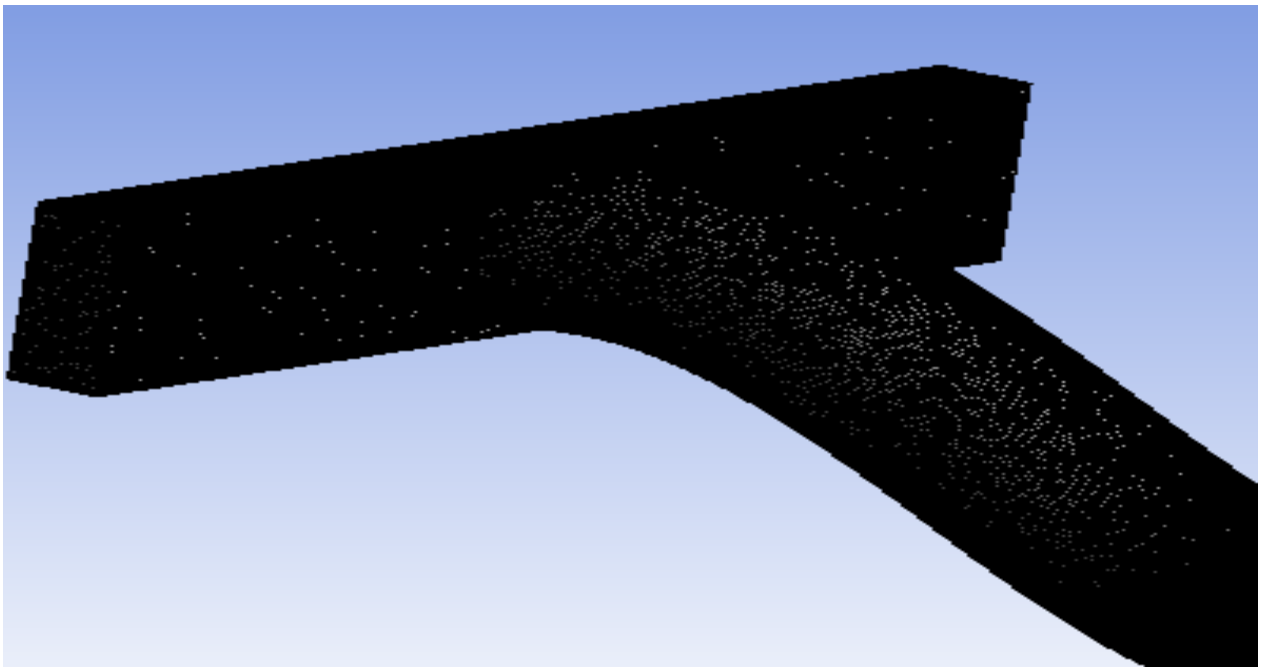

Fig.4.2 Mesh of spiral T shape

The details of the meshing module generated above are elaborately given below which are obtained in ANSYS meshing in Table 4.2.

Table 4.2 Mesh details of spiral T shape micromixer

File Name	Mesh
Physics Technique	CFD
Solver Used	Fluent
Relevance	0
Element Order	Linear
Size Nature	Adaptive
Center of Relevance	Fine
Element Size	3.0 µm
Initial Size Seed	Assembly
Transition	Slow

Span Angle Center	Fine
Automatic Mesh-based Defeaturing	On
Minimum Edge Length	62.6660 µm
Default Skewness	0.90
Smoothing	Medium
Mesh Metric	Orthogonal Quality
Average	0.76501
Standard Deviation	0.12096
Inflation Option	Smooth Transition
Transition Ratio	0.272
Maximum Layers	5
Growth Rate	1.2
Inflation Algorithm	Pre
View Advanced Options	No
Method	None
Number of CPUs for the Meshing	Program Controlled
Rigid Body Behavior	Dimensionally Reduced
Mesh Morphing	Disabled
Triangle Surface Mesher	Program Controlled
Generate Pinch on Refresh	No
Nodes	475017
Elements	2455174

The mesh was generated using the adaptive option with the optimum sizing. For the spiral T shaped micromixer, the mesh was created as a structured mesh and for checking the solutions the mesh

was made finer and the solutions obtained were meshing independent. After the meshing, the geometry is labelled in the form of desired inlets, outlets and periphery.

4.5 Setup Details

The setup is generated in parallel version mode with the number of processors set as 4. In the setup details, after the generation and mesh display of the model, the species transport phenomenon is turned on and applied. From the materials option available in the tree, add water and dye in the fluid domain from the FLUENT database. The desired fluids namely; water and dye need to be inserted in the species transport option.

The water and dye are then added in the mixing domain species and others are removed. The energy equation needs to be turned off as we are not considering thermal effects. The values for this mixing species model is then provided. Then the boundary conditions are defined for the simulation model. The method used for the simulation is SIMPLEC. Then the convergence limit is edited and set as of the order of 1e-08. All the details are given below regarding boundary conditions in Table 4.3.

Table 4.3 Boundary conditions

Material	Water	Dye
Reynolds number, Re	266	266
Velocity specification method	Normal to boundary	Normal to boundary
Velocity, V (m/s)	1.67	1.67
Mass fraction (inlet1)	1	0
Mass fraction (inlet2)	0	1
Initial gauge pressure (kpa)	0	0
Convergence criteria	1e-08	1e-08

Then the standard initialization is done which is computed from all zones and the reference frame is set to relative to cell zone. After this, the calculation setup details are filled and this simulation is observed until it reaches about 2000 iterations. The simulation results obtained are then analyzed and calculated. The results obtained are discussed in detail in chapter 6.

CHAPTER 5

METHODOLOGY (II)

SPIRAL T MICROMIXER (WITH NANOFLUID)

The same numerical model of Spiral T shaped micromixer is used for the mathematical evaluation of mixing index using Nanofluid (Al_2O_3). Water is taken as the base fluid during the whole analysis. During the complete investigation, we have considered only 1% (volume fraction in pure water) concentration of the nanofluid. The given nanofluid is considered as the sole phase fluid and is allowed to flow through one of the inlets of the spiral T micromixer. At the other inlet, pure water is given as another fluid. The two fluids are allowed to mix together in the circular cross-section of the spiral. Their mixing behavior is analyzed throughout the spiral mixing channel and mass fraction contours are obtained. The mixing performance characteristic is determined in terms of the mixing index.

5.1 Properties of the Nanofluids

The properties of the base fluid and solid particles, their volume fraction in the suspension and its shape decide the thermo-physical properties of the nanofluids. The nanofluids properties can be defined by the relations given below in Equation (5.1) and Equation (5.2) according to the reference Tsai et al. (2007), Lee et al. (2007) [43, 44].

Viscosity;

$$\mu_{nf} = \mu_{f\,(}1+2.5c) \tag{5.1}$$

Density;

$$\rho_{nf} = c\rho_p + (1\text{-}c)\,\rho_f \tag{5.2}$$

ρ_f, ρ_{nf}, ρ_p are stated as densities of the base fluid, nanoparticles and the solid particles respectively and the same subscripts are used for viscosities also. The properties of the nanofluid according to reference Chen et al. (2007) [45] used are given below in Table 5.1.

Table 5.1 Thermo-physical properties of the nanofluid [45]

Material	**ρ** **(kg/m^3)**	**μ** **(kg/m.s)**
Pure water (c=0%)	981.3	0.000598
Al_2O_3-water (c=1%)	1007.4	0.000612

5.2 Preparation of Nanofluid

For the nanofluid preparation, the widely accepted procedure is a dual-step preparation process. In this method, nanofluid is prepared by mixing base fluid with available nanopowders commercially. These nanopowders are obtained from various physical, mechanical and chemical methods like milling, grinding, and sol-gel and vapor-phase methods. The viable mixing of nano powders and base fluid is achieved by high order shear mixing device or an ultrasonic vibrator. Accumulation of powder because of high Van der Walls attraction force between nanoparticles affects its stability, which is the major drawback of this two-step operation. But still, this process is most economic and approved for the production of nanofluids in spite of its disadvantages. The widely used two-step method is shown below (Fig.5.1).

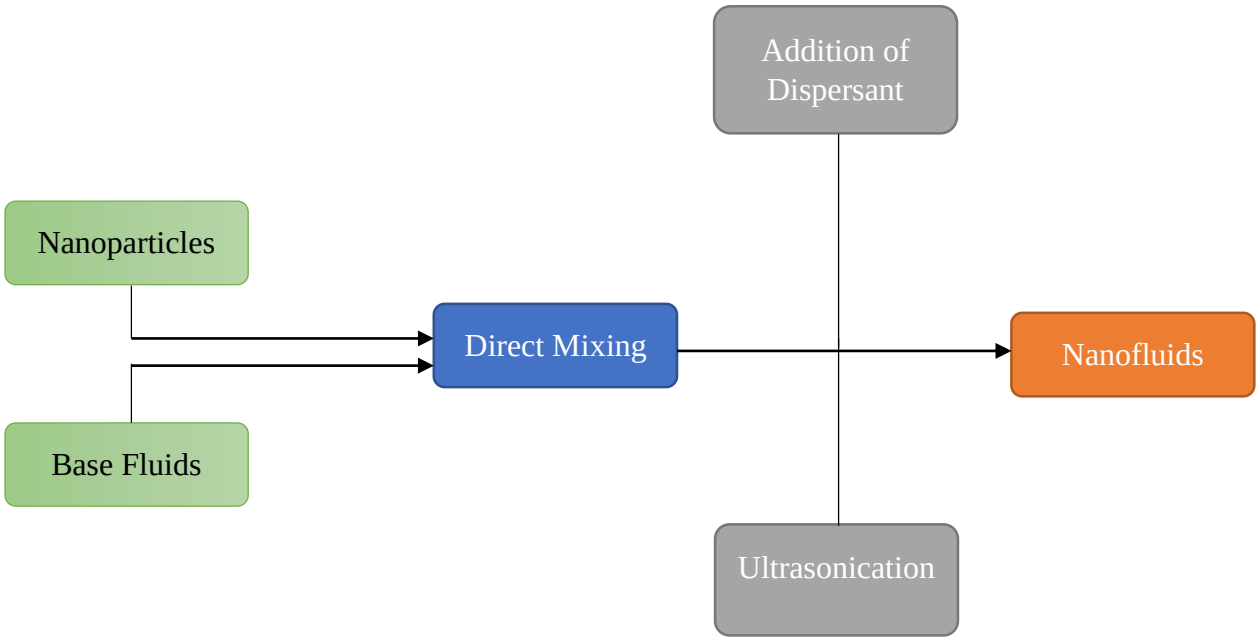

Fig.5.1 Two-step preparation process of nanofluid

5.3 Description of the Problem

In order to further increase the micromixing efficiency of two fluids with different thermo-physical properties, this additional research has been carried out. There are many active and passive micromixers of different geometries and different innovative structural developments. In this section, we will observe and numerically simulate the mixing efficiency of the two fluids, namely; water and nanofluid inside the Spiral T shape passive micromixer. Then, we will compare the obtained results with that of the simple T shape passive micromixer of the same volumetric size and with spiral T shape passive micromixer without nanofluid.

5.4 Geometrical Construction and Specifications

The specifications of the Spiral T shape passive micromixer is same as given in the section 4.3 and 4.4. The details of this micromixer geometry are given below in Table 5.2. The same geometry is fabricated in Solidworks and then imported to ANSYS workbench using supported formats.

Table 5.2 Geometrical dimensions

Type	**Spiral T shape** **(Dimensions)***
Inlet cross section	159.5769*62.6657
Non mixing channel length	800
Mixing channel diameter(d_h)	159.5769
Mixing channel length	~3000
Spiral Diameter (D)	400
Spiral Pitch (p)	2000
Spiral Turns (n)	~1.25

5.5 Meshing

The meshing details are also the same as specified in section 4.4. The same meshing module is incorporated for this model. After the meshing operation, only the dye inlet is edited to the nanofluid inlet and the rest remains the same. The details of the mesh are already mentioned in section 4.4 in Table 4.2.

5.6 Setup Details

In the setup details, after the generation of the model, the species transport phenomenon is turned on and applied. From the materials option, add water and nanofluid and their properties are filled according to the reference Hasan et al. (2012) [46] in the fluid domain. The desired fluids namely; water and nanofluid need to be inserted in the species transport option. The energy equation option needs to be turned off as we are not considering the effects of thermal conductivity variation. The water and nanofluid are then added in the mixing domain species and others are removed. The

energy equation needs to be turned off as we are not considering thermal effects. The values for this mixing species model is then provided. Then the boundary conditions are defined for the simulation model. The method used for the simulation is SIMPLEC. Then the convergence limit is edited and set as of the order of 1e-08. All the boundary conditions details are given below in Table 5.3.

Table 5.3 Boundary conditions for water-nanofluid

Material	Water	Nanofluid(1%Al_2O_3)
Reynolds number, Re	266	266
Velocity specification method	Normal to boundary	Normal to boundary
Velocity, V (m/s)	1.67	1.67
Mass fraction (inlet1)	1	0
Mass fraction (inlet2)	0	1
Initial gauge pressure (kpa)	0	0
Convergence criteria	1e-08	1e-08

CHAPTER 6

VALIDATION

The validation and analysis of T shape passive micromixer is performed on commercial software, ANSYS workbench which analyzes the diffusion and flows in the microchannel. There are several numerical and experimental analysis of flow and mixing regimes of two fluids performed earlier with the identical thermo-physical properties in T shape micromixers. During the researches of the mixing process, the flow regimes that are revealed are five i.e. (a) stationary vortex flow (b) stationary symmetric vortex flow (c) stationary asymmetric vortex flow (engulfment regime) (c) unsteady periodic flow (d) stochastic flow (e) laminar to turbulent transition. However, a significant increment in the efficiency of mixing at the transition to asymmetric from the symmetric mode for a stationary regime of flow (called the engulfment regime) is observed in most of the researches carried out. The above-stated regime is of utmost interest as the mixing efficiency increases promptly in this section. In this paper, we have taken two different fluids, namely; water and dye (almost similar properties as of water), and the same regime pattern go for it. The simulation results obtained are then validated with the reference Dundi et al. (2016) [47]. The properties of water and dye are given below are added from the fluent database in Table 6.1.

Table 6.1 Water-dye properties

Material	**Density (kg/m^3)**	**Viscosity (kg/m.s)**	**Diffusivity (m^2/s)**
Water	998.2	0.001	2e-09
Dye	≈ 998.2	≈ 0.001	2e-09

6.1 Geometry Specifications

The T shape micromixers are of the simplest type in micromixing phenomenon. The numerical investigation has already been conducted for the mixing of different fluids with different thermo-physical properties by many researchers. The two fluids mixing characteristics are observed at different Re. In this case, we have taken the mixing index as the validating criteria. The geometry of the T shape passive micromixer is fabricated in commercial solid modeling CAD software Solid works by Dassault Systèmes. The details of the structure of geometry are given below (Fig.6.1).

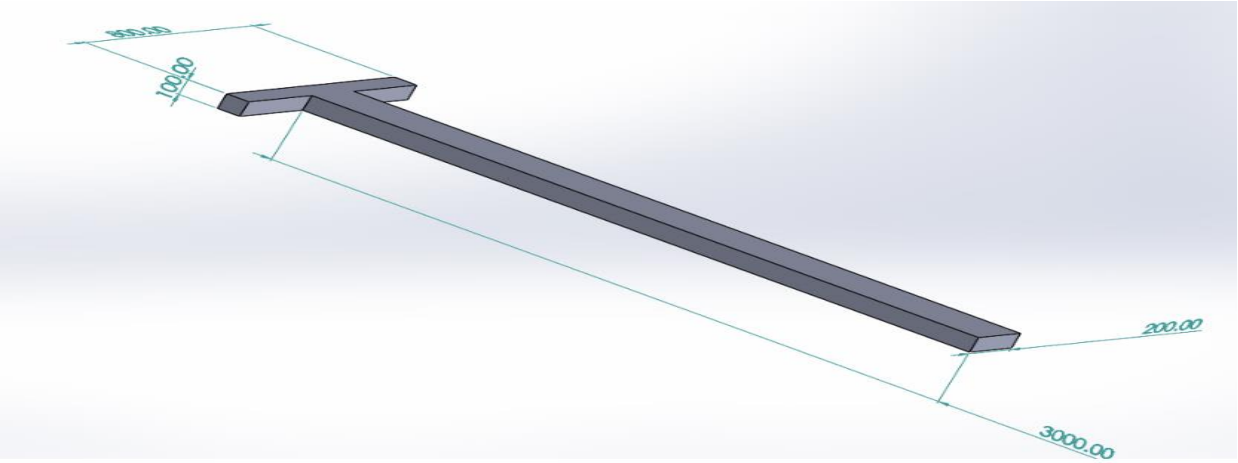

Fig.6.1 Simple T shape micromixer

6.2 Numerical Simulation Result Validation

The above geometry shown above then has been imported to ANSYS Fluent software for validation using supported formats. The computational simulation results have been obtained for the given geometry and compared to the one we are validating with. At Re= 266, the mass contour for water-dye at the outlet in the reference paper (Fig. 6.2(a)) and the computational result is given below (Fig. 6.2(b)).

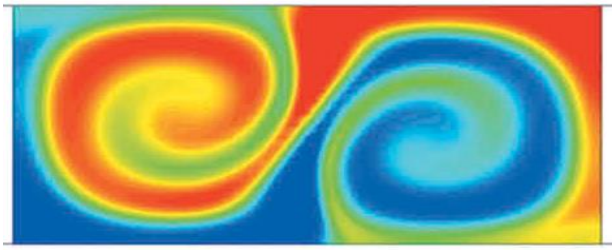

(a)

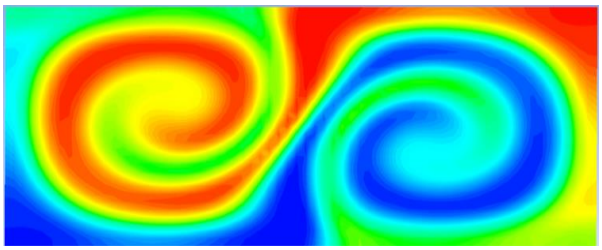

(b)

Fig.6.2 Comparison of the mass fraction contours of water-dye at the outlets of simple T micromixer **(a)** Reference paper [47] **(b)** Computational simulation at Re=266

6.3 Mixing Index calculation

During the fusion of phases, the concentration of a species at one side of the channel will be reduced from 1, while on the other side it will increase from 0. The mixing efficiency is typically calculated by computing the deviation from the perfect mixing according to the reference Jain et al. (2013) [48], as shown in Equation (6.1). The deviation of the concentration should be zero for uniform mixing with a mixing index of one. On the contrary, a lesser amount of mixing is achieved as the mixing index starts to decrease from 1. In Equation (6.1), N is the number of sample points in the selected cross-sectional area used for calculation of the mixing index, η. The parameter c denotes the scaled concentration value at that point, while $\bar{c}^*$ and $\bar{c}^0$ are the scaled concentration with perfect mixing at each point (i.e.0.5) and when the solutions are unmixed, respectively.

$$\eta = 1 - \sqrt{\frac{\left(\frac{\sum_{n=1}^{N}(\bar{c} - \bar{c}^{*})^{2}}{N}\right)}{\left(\frac{\sum_{n=1}^{N}(\bar{c}^{o} - \bar{c}^{*})^{2}}{N}\right)}} \tag{6.1}$$

The Mixing indices calculated for the micromixers at the outlet at the given Re=266 at their respective outlet (Fig.6.2) are given below in Table 6.2.

Table 6.2 Mixing index comparison at Re=266

Reynolds number	**Reference paper [47]**	**Computational simulation**
266	0.328	0.35484

The mixing index in form of a bar chart is also obtained for our computational simulated simple T shape micromixer alongside reference simple T shape passive micromixer at Re = 266 (Fig. 6.3).

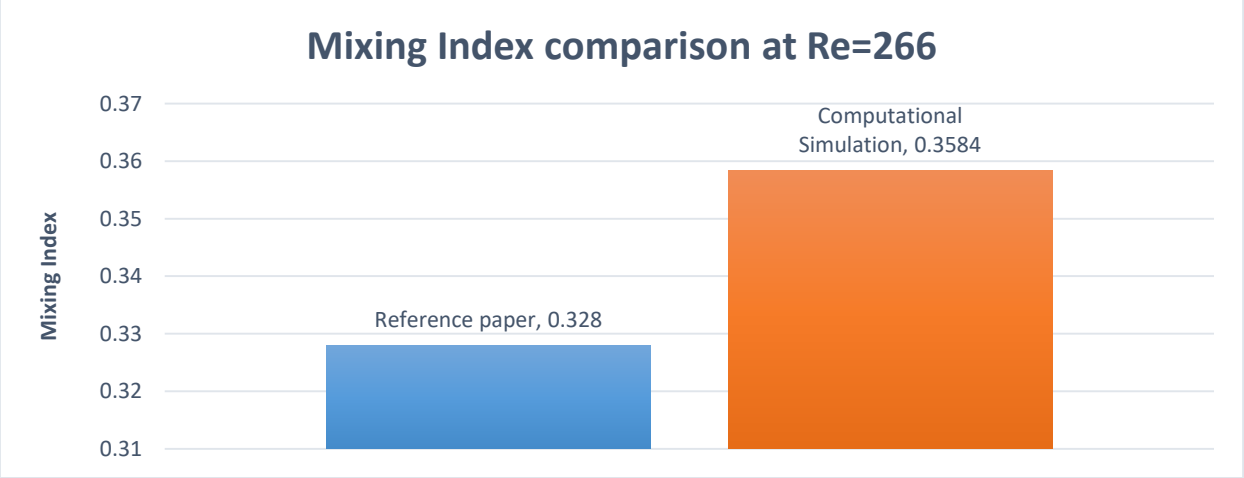

Fig.6.3 Mixing index comparison

For validating purposes, mixing indices at different locations for water-dye has been observed and the results have been compared. The data comparison has been plotted in the graphical form (Fig 6.4).

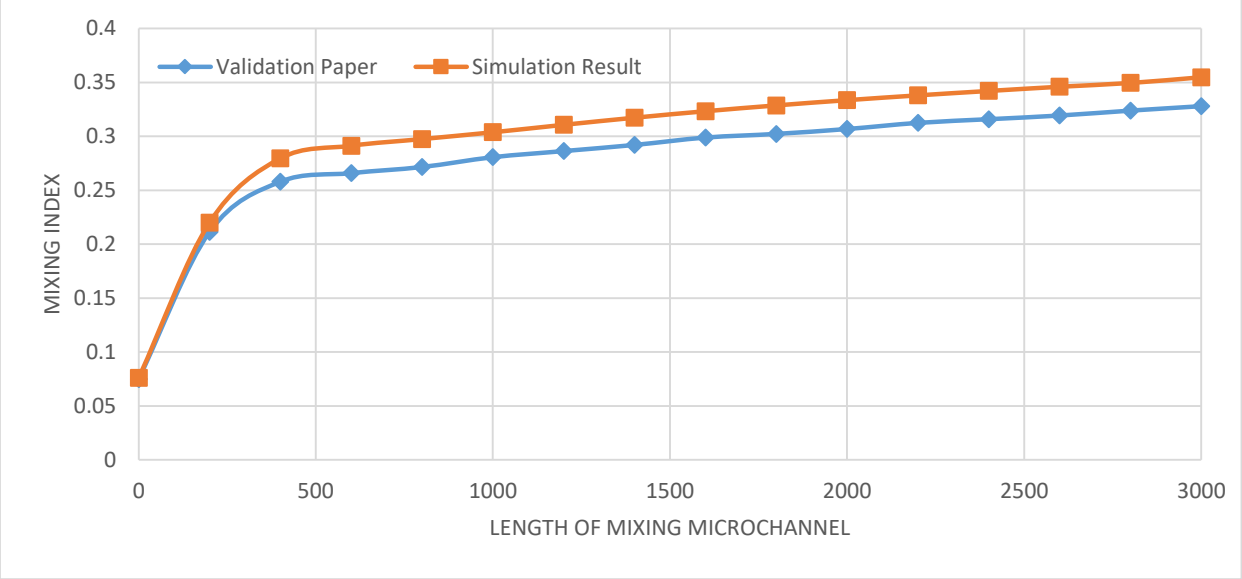

Fig.6.4 Mixing Index comparison of simple T shape Micromixers

The two fluids when entered the micromixing channel, they try to mix with each other. The blue color in the channel denotes the mass fraction of water whereas the red color denotes the mass fraction of dye. The mixing mass contours are observed, each at a distance of 100µm from other contour plane, in the mixing channel (Fig.6.5).

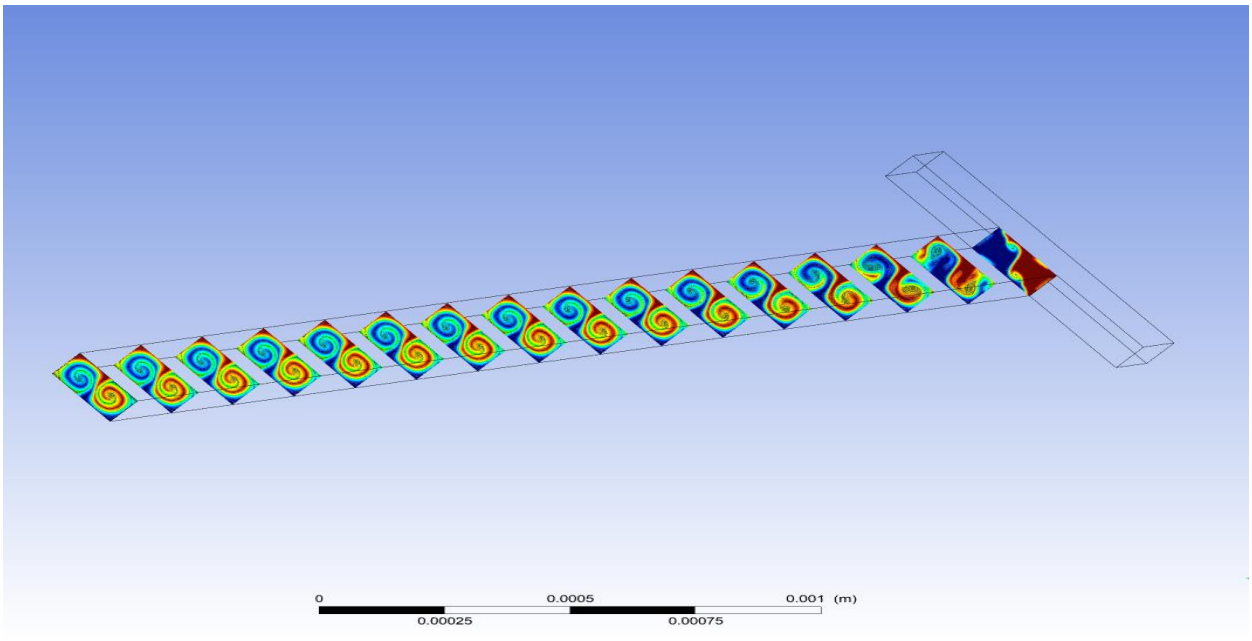

Fig.6.5 Mass fraction contours of mixing of water-dye at Re=266 at different locations inside the simple T shape Micromixer

From the above data, we have observed that the mass fraction contours obtained after computational simulation are almost the reflection of the validating model and also the mixing index of computational simulation is very much compatible and under the limits of prescribed validation.

CHAPTER 7

SIMULATION RESULTS

The simulation results obtained after running the setup for about 2000 iterations for the simple T shape, spiral T shape without nanofluid and spiral T shape with nanofluid are discussed below. The results obtained after finishing off set up files are the main objectives of the CFD simulation. The types of results achieved from a CFD simulation are quantities of engineering interest in the observed flow case. The micromixing efficiency is the bone of contention for the above computational analysis.

7.1 Spiral T Shape Micromixer without Nanofluid

The two fluids are allowed to fuse into one another and their mixing behavior at different Re has been observed. In the reference paper, Mass fractions contours and Mixing Index is calculated at Re=266 for T shape passive micromixer, so we need to compute that for spiral T shape Micromixer also.

Firstly the mass fraction contours have been observed and compared throughout the channel at Re=266 for T shape and Spiral shape (Fig.7.1 (a) and (b)).

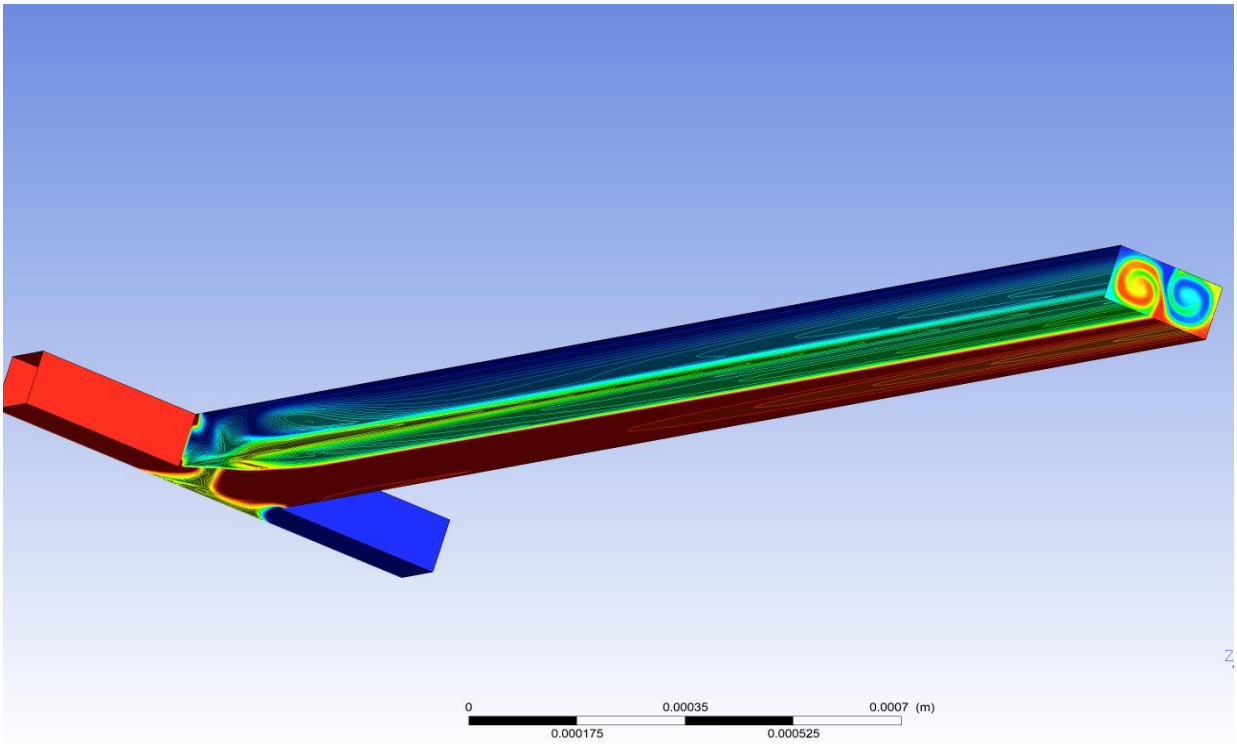

(a)

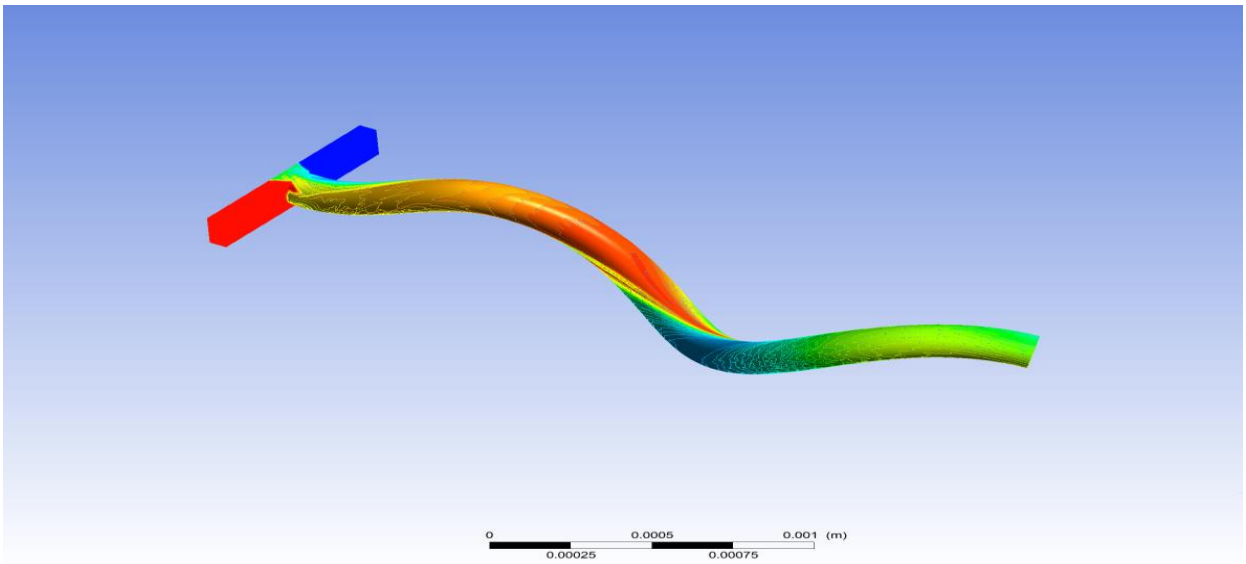

(b)

Fig.7.1 Mass fraction contour comparison of water-dye inside the **(a)** Simple T shape and **(b)** Spiral T shape (without nanofluid) passive micromixers

The mass fraction contour is observed and analyzed at the outlet of the micromixers (Fig.7.2).

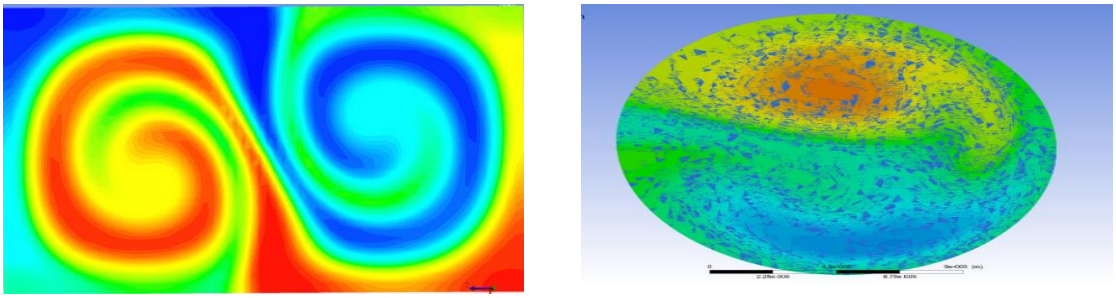

(a) **(b)**

Fig.7.2 Comparison of mass fraction contours of water-dye at the outlets of **(a) S**imple T shape and **(b)** Spiral T shape respectively at Re=266

Secondly, the Mixing Index at the outlet for simple T shape and spiral T shape micromixers has been analyzed and compared at Re=266 (Fig.7.3)

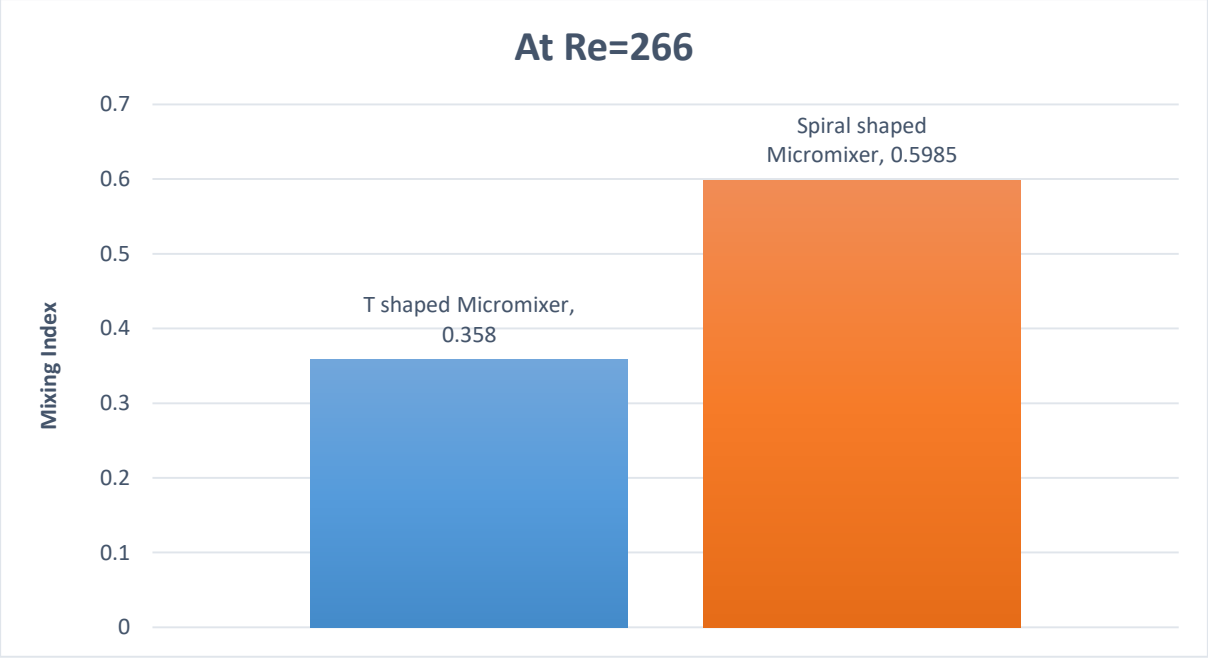

Fig.7.3 Comparison of simple T and spiral T shape micromixer at Re = 266

Then the Mixing Indices have been calculated for Spiral shape at various Re at the outlet zone of the micromixer. The pattern of the mixing efficiency is observed with the increase in Reynolds number (Fig.7.4).

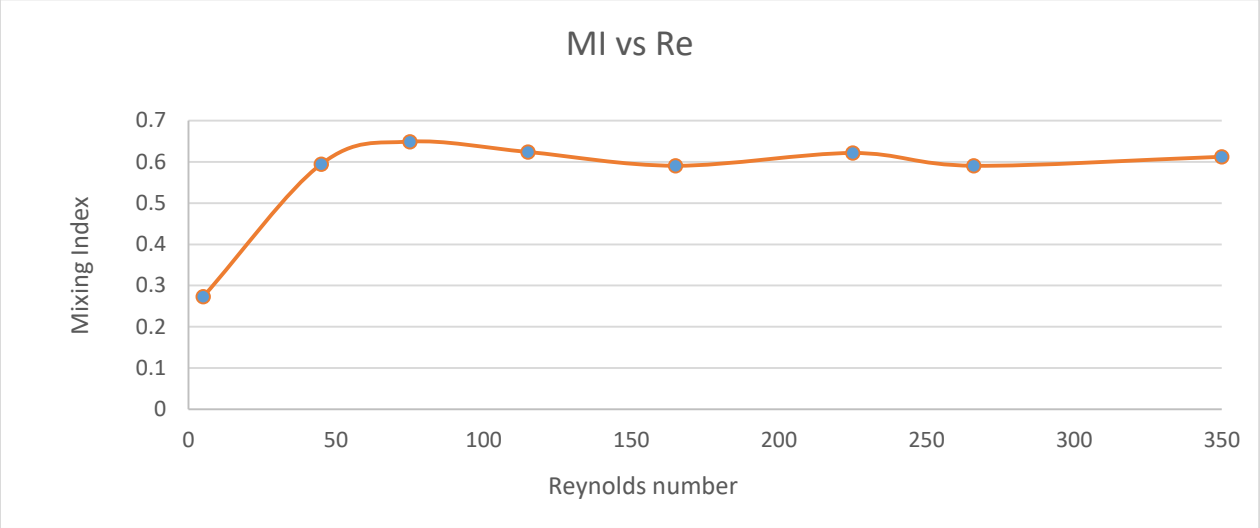

Fig.7.4 Mixing Index variation at various Re in a spiral T shape passive micromixer (without nanofluid).

The comparison of mixing index with its neighboring Reynolds number is shown below in form of bars (Fig.7.5).

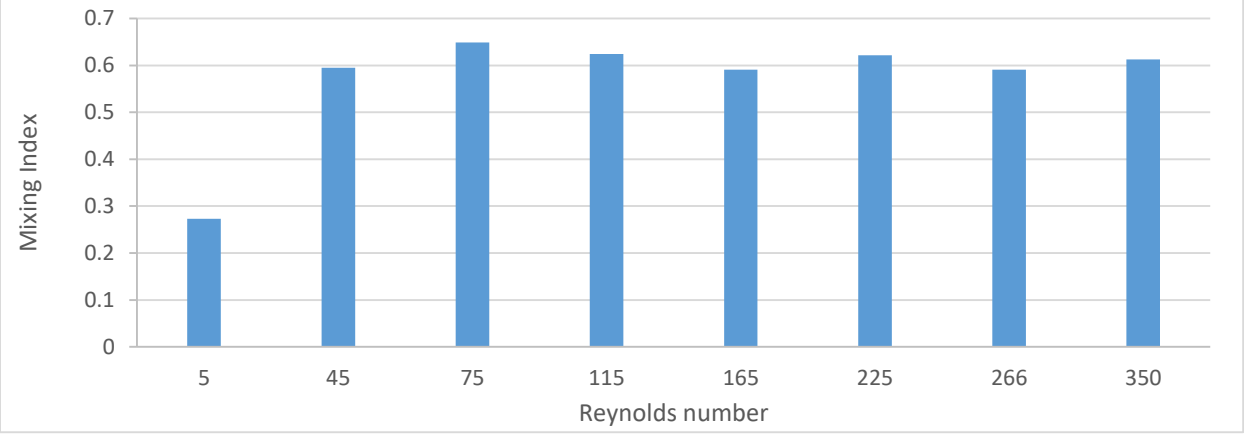

Fig.7.5 Values of Mixing Index at various Re

The main focus of this research is to enhance the mixing performance. So, we need to compare the mixing index at outlets with the reference simple T shape micromixer. The above variation of the mixing efficiency is then compared with the simple T shape micromixer in the form of continuous graphical form at the above specified Re (Fig.7.6).

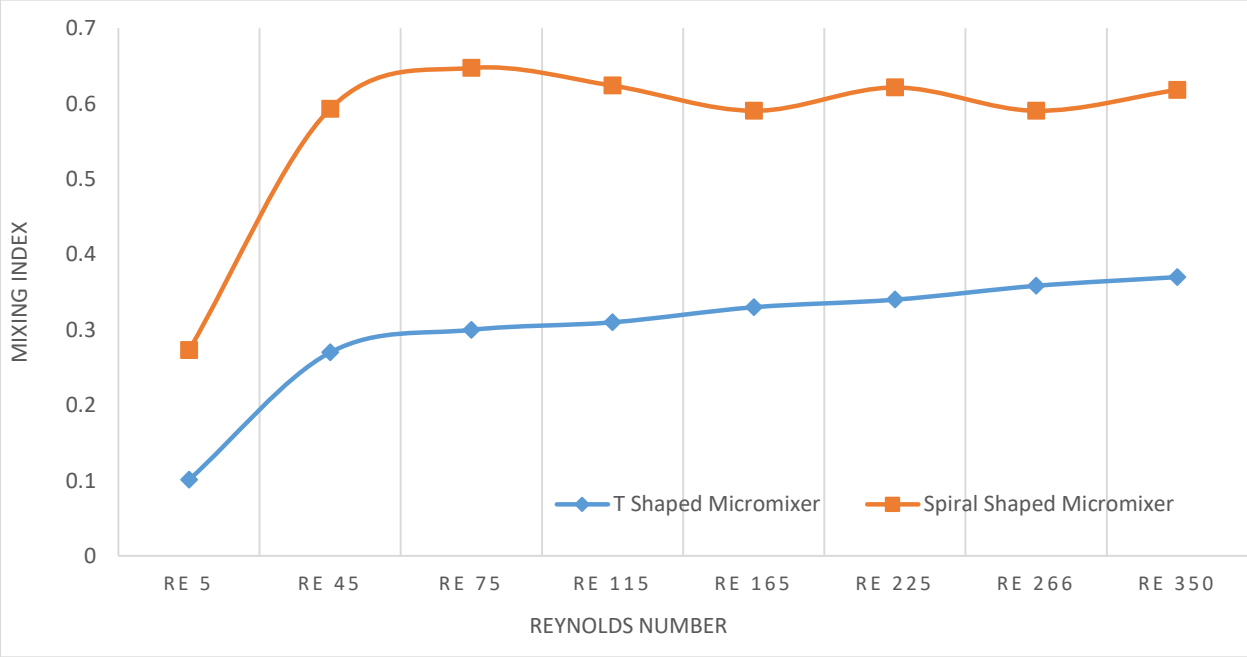

Fig.7.6 Mixing Index comparison at the outlets

7.2 Spiral T Shape Micromixer with Nanofluid

The spiral T shape with one of the inlet fluids as nanofluid is numerically investigated and its performance is compared with simple T shape and spiral T (without nanofluid). Firstly, the mass contour of spiral T with nanofluid has been obtained at Re=266 (Fig.7.2.1).

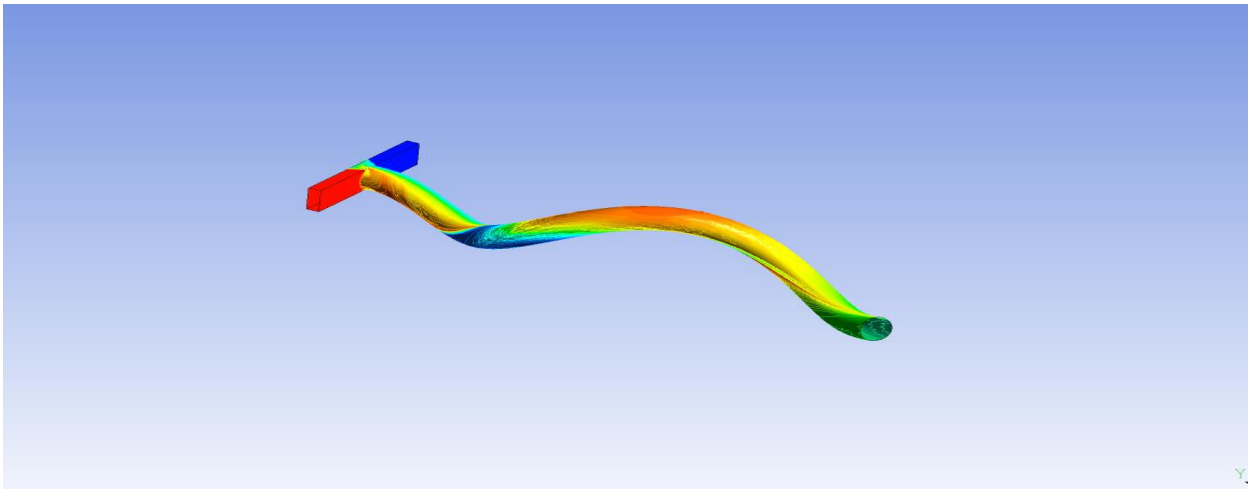

Fig.7.2.1 Mass fraction contour of water-nanofluid (1% Al_2O_3) at Re=266

Secondly, the mass fraction contour of the above-stated micromixer is obtained and compared with the other micromixer. The mass fraction contours at the outlet of the three micromixers are given and compared below (Fig.7.2.2).

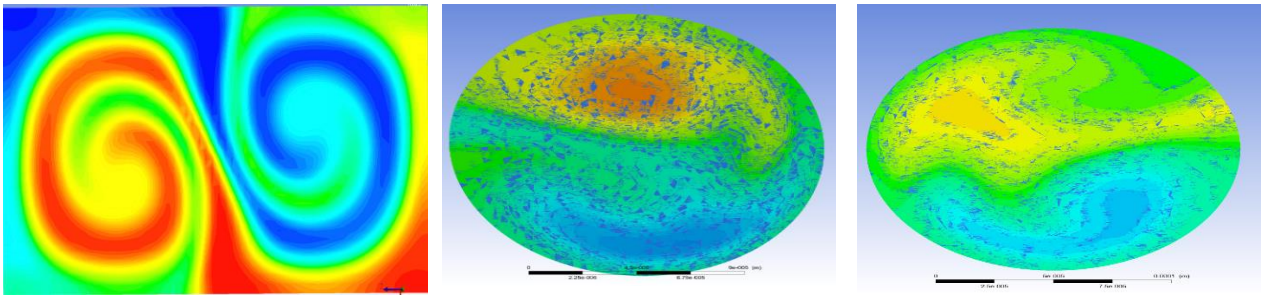

(a) **(b)** **(c)**

Fig.7.2.2 Comparison of mass fraction contours of **(a)** Simple T shape **(b)** Spiral T shape (without nanofluid) **(c)** Spiral T shape (with nanofluid) passive micromixers at Re=266.

The performance of the mixing of the fluids is first compared at Reynolds number of 266. It is taken as the default case. We already have the mixing index values of simple T shape and spiral T shape (without nanofluid) at Re = 266. So, we have calculated the value of mixing index at the same Reynolds number for spiral T shape (with nanofluid). The mixing index of the three micromixers at Reynolds number 266 is shown and compared below in the form of bar charts (Fig.7.2.3).

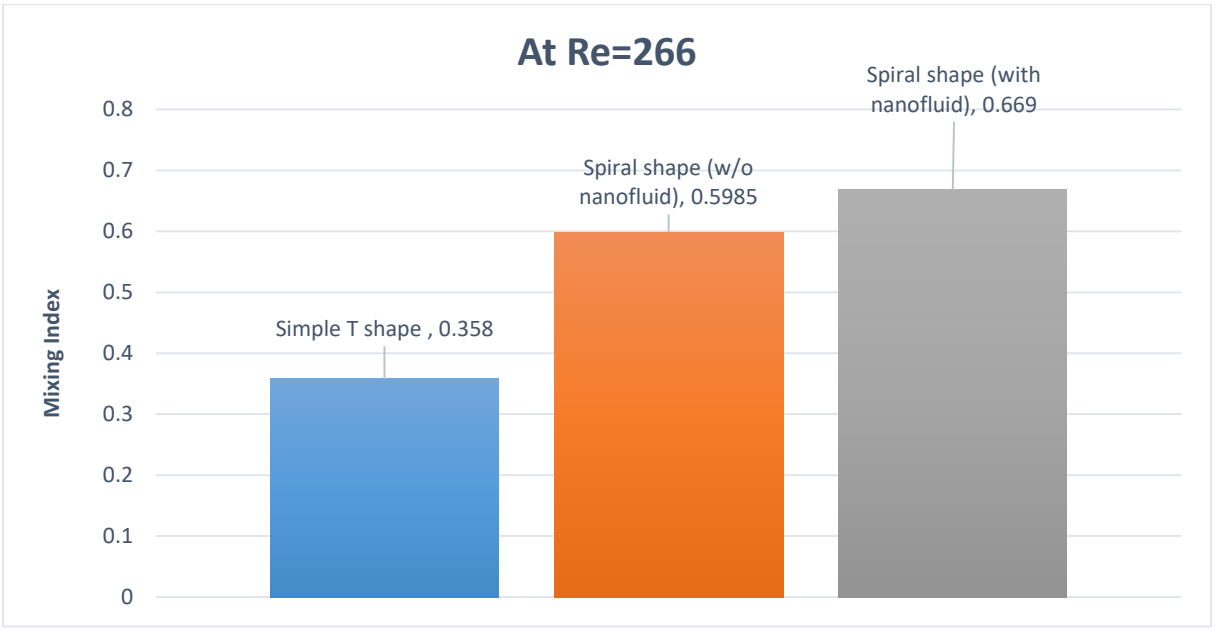

Fig.7.2.3 Comparison of mixing index of three passive micromixing modules at Re=266

Then the mixing index at the outlet for the spiral T micromixer (with nanofluid) for the mixture of water-nanofluid (1% Al_2O_3) is obtained for a wide variety of Reynolds number. The Reynolds number is varied from 5 to 350 to check the feasibility of this type of module (Fig.7.2.4).

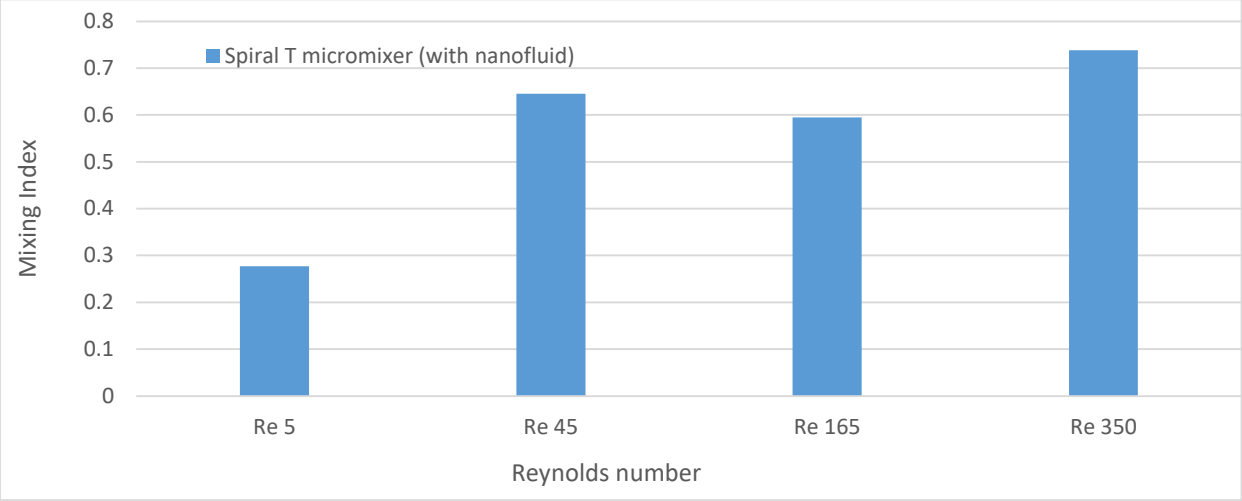

Fig.7.2.4 Mixing index values at different Reynolds number (with nanofluid)

Though an appreciable enhancement is observed in the mixing index in this type of micromixer, but it is also observed that there is a decrease in the mixing index at Re = 165. Even from the Fig.7.2.3, we can observe that at Re = 266, the micromixing index for this micromixer shows a better performance from the values of Re < 266.

7.3 Comparison of the Mixing Index Inside Simple T, Spiral T (with and without Nanofluid) Passive Micromixers

The mixing performance is then compared with spiral T shape without nanofluid and also with simple T shape passive micromixers at the same Reynolds numbers. The mixing index is plotted against the Reynolds number (Fig.7.3.1).

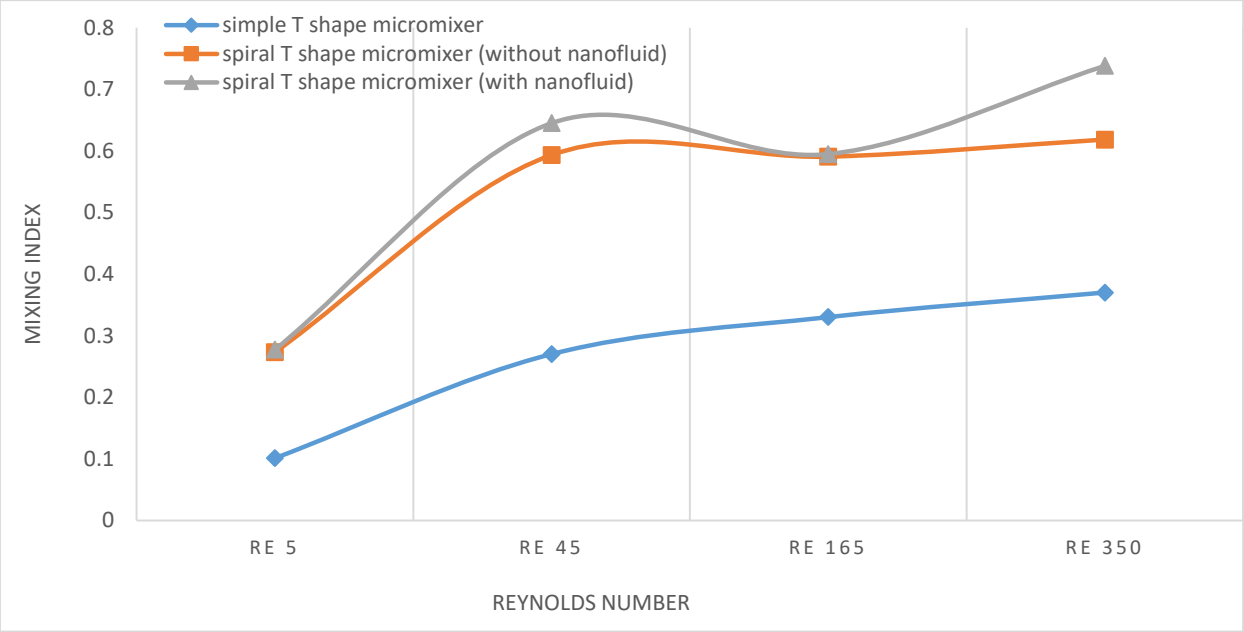

Fig.7.3.1 Mixing Index variation of simple T, spiral T (without nanofluid) and spiral T (with nanofluid) respectively at Re 5, 45, 165, 350.

From the above-plotted graphs, the below points are observed:

- The minimum value of the mixing index amongst the different types of passive micromixer is observed at Re= 5 for simple T shape micromixer, and its value is 0.101.
- The maximum value of mixing index amongst the different types of passive micromixer is observed at Re= 350 for spiral T shape (with nanofluid) micromixer and its value is 0.738.
- At low values of Reynolds number (5 < Re < 45), the spiral T shape micromixer both with and without nanofluid almost coincides with each other but for higher values of Reynolds number micromixer with nanofluid possesses better mixing performance.

- Though, it can be seen from the above graphs that the mixing index decreases in the mid-range of provided Re for spiral T shape micromixers because of lesser residence time for the diffusion of fluid particles with increment in the flow velocity. But, afterward, the increase in Reynolds numbers tends to generate swirling effects according to the reference Engler et al. (2004) [49]. If the micromixer geometry stimulates these swirling effects, then fluid path stretching can compensate for a reduction in residence time.

CONCLUSIONS

In this research paper, a numerical investigation is carried out between simple T shape, spiral T shape without nanofluid and spiral T shape with nanofluid passive micromixers. From the simulation results, it can be concluded that both the spiral T passive micromixer without nanofluid and with nanofluid show much better mixing performance than the simple T passive micromixer at each Reynolds number. It could be due to the presence of a swirling effect in spiral passive micromixers that the mixing index increases.

Although both the Spiral T shape without nanofluid and with nanofluid shows the same results at low Reynolds number ranging from $5 < Re < 45$, but, as the Reynolds goes beyond 40, the spiral T shape micromixer with nanofluid shows better mixing results than the other two.

So, we can say that with the use of a particular concentration of stated nanofluid, we can enhance the mixing performance at the specified Reynolds numbers. It is evident from the analyzed data that the mixing index for above-stated micromixer with nanofluid enhances at higher Reynolds numbers. This shows that the nanofluid addition (1% Al_2O_3 concentration to base fluid water) exhibits better miscibility with water than the other stated cases.

Therefore, just by modifying the basic T shape micromixer geometry to spiral T shape, we can achieve much better mixing performance with the same boundary conditions.

REFERENCES

[1] Ansari, Mubashshir A., Kwang-Yong Kim, Khalid Anwar, and Sun Min Kim. "Vortex micro T-mixer with non-aligned inputs." *Chemical Engineering Journal* 181 (2012): 846-850.

[2] Hossain, Shakhawat, M. A. Ansari, and Kwang-Yong Kim. "Evaluation of the mixing performance of three passive micromixers." *Chemical Engineering Journal* 150, no. 2-3 (2009): 492-501.

[3] Ansari, Mubashshir Ahmad. "Parametric study on mixing of two fluids in a three-dimensional serpentine microchannel." *Chemical Engineering Journal* 146, no. 3 (2009): 439-448.

[4] Chen, Yao, and Xueye Chen. "An improved design for passive micromixer based on topology optimization method." *Chemical Physics Letters* 734 (2019): 136706.

[5] Vijayanandh, Vidhya, Aarathi Pradeep, P. V. Suneesh, and TG Satheesh Babu. "Design and simulation of passive micromixers with ridges for enhanced efficiency." In *IOP Conference Series: Materials Science and Engineering*, vol. 577, no. 1, p. 012106. IOP Publishing, 2019.

[6] Shah, Imran, Han Su Jeon, Muhsin Ali, Doh Hoi Yang, and Kyung-Hyun Choi. "Optimal parametric mixing analysis of active and passive micromixers using Taguchi method." *Proceedings of the Institution of Mechanical Engineers, Part E: Journal of Process Mechanical Engineering* 233, no. 6 (2019): 1292-1303.

[7] Lobasov, Alexander S., Anna A. Shebeleva, and Andrey V. Minakov. "The study of ethanol and water mixing modes in the T-shaped micromixers." *Журнал Сибирского федерального университета. Математика и физика* 12, no. 2 (2019).

[8] Hossain, Shakhawat, Insu Lee, Sun Min Kim, and Kwang-Yong Kim. "A micromixer with two-layer serpentine crossing channels having excellent mixing performance at low Reynolds numbers." *Chemical Engineering Journal* 327 (2017): 268-277.

[9] Chen, Xueye, and Tiechuan Li. "A novel passive micromixer designed by applying an optimization algorithm to the zigzag microchannel." *Chemical Engineering Journal* 313 (2017): 1406-1414.

[10] Chen, Xueye, and Tiechuan Li. "A novel design for passive misscromixers based on topology optimization method." *Biomedical microdevices* 18, no. 4 (2016): 57.

[11] Viktorov, Vladimir, Md Readul Mahmud, and Carmen Visconte. "Numerical study of fluid mixing at different inlet flow-rate ratios in Tear-drop and Chain micromixers compared to a new HC passive micromixer." *Engineering Applications of Computational Fluid Mechanics* 10, no. 1 (2016): 182-192.

[12] Li, Xiaoping, Honglong Chang, Xiaocheng Liu, Fang Ye, and Weizheng Yuan. "A 3-D overbridge-shaped micromixer for fast mixing over a wide range of reynolds numbers." *Journal of Microelectromechanical Systems* 24, no. 5 (2015): 1391-1399.

[13] Ta, Bao Quoc, Hoà Lê Thanh, Tao Dong, Trung Nguyen Thoi, and Frank Karlsen. "Geometric effects on mixing performance in a novel passive micromixer with trapezoidal-zigzag channels." *Journal of Micromechanics and Microengineering* 25, no. 9 (2015): 094004.

[14] Yang, An-Shik, Feng-Chao Chuang, Chi-Kuan Chen, Mei-Hui Lee, Shih-Wei Chen, Tsai-Lung Su, and Yung-Chun Yang. "A high-performance micromixer using three-dimensional Tesla structures for bio-applications." *Chemical Engineering Journal* 263 (2015): 444-451.

[15] Andreussi, Tommaso, Chiara Galletti, Roberto Mauri, Simone Camarri, and Maria Vittoria Salvetti. "Flow regimes in T-shaped micro-mixers." *Computers & Chemical Engineering* 76 (2015): 150-159.

[16] Rasouli, M. R., A. Abouei Mehrizi, and A. Lashkaripour. "Numerical study on low Reynolds mixing oft-shaped micro-mixers with obstacles." *Transp Phenom Nano Micro Scales* 3, no. 2 (2015): 68-76.

[17] Liu, Keyin, Qing Yang, Feng Chen, Yulong Zhao, Xiangwei Meng, Chao Shan, and Yanyang Li. "Design and analysis of the cross-linked dual helical micromixer for rapid mixing at low Reynolds numbers." *Microfluidics and nanofluidics* 19, no. 1 (2015): 169-180.

[18] Le The, Hai, Nhut Tran-Minh, Hoa Le-Thanh, and Frank Karlsen. "A novel micromixer with multimixing mechanisms for high mixing efficiency at low Reynolds number." In *The 9th IEEE International Conference on Nano/Micro Engineered and Molecular Systems (NEMS)*, pp. 651-654. IEEE, 2014.

[19] Le The, Hai, Hoa Le-Thanh, Nhut Tran-Minh, and Frank Karlsen. "A novel passive micromixer with trapezoidal blades for high mixing efficiency at low Reynolds number flow." In *2nd Middle East Conference on Biomedical Engineering*, pp. 25-28. IEEE, 2014.

[20] Tran-Minh, Nhut, Tao Dong, and Frank Karlsen. "An efficient passive planar micromixer with ellipse-like micropillars for continuous mixing of human blood." *Computer methods and programs in biomedicine* 117, no. 1 (2014): 20-29.

[21] Afzal, Arshad, and Kwang-Yong Kim. "Multi-objective optimization of a passive micromixer based on periodic variation of velocity profile." *Chemical engineering communications* 202, no. 3 (2015): 322-331.

[22] He, X., D. Wei, Z. Deng, S. Yang, and S. Cai. "Mixing performance of a novel passive micromixer with logarithmic spiral channel." *J. Drainage Irrigation Mach. Eng.* 32, no. 11 (2014): 968-972.

[23] Hossain, Shakhawat, and Kwang-Yong Kim. "Mixing analysis of passive micromixer with unbalanced three-split rhombic sub-channels." *Micromachines* 5, no. 4 (2014): 913-928.

[24] Li, Jian, Guodong Xia, and Yifan Li. "Numerical and experimental analyses of planar asymmetric split-and-recombine micromixer with dislocation sub-channels." *Journal of Chemical Technology & Biotechnology* 88, no. 9 (2013): 1757-1765.

[25] Wang, Lei, Shenghua Ma, Xuejing Wang, Hongmei Bi, and Xiaojun Han. "Mixing enhancement of a passive microfluidic mixer containing triangle baffles." *Asia-Pacific Journal of Chemical Engineering* 9, no. 6 (2014): 877-885.

[26] Alam, Afroz, Arshad Afzal, and Kwang-Yong Kim. "Mixing performance of a planar micromixer with circular obstructions in a curved microchannel." *Chemical Engineering Research and Design* 92, no. 3 (2014): 423-434.

[27] Wu, Chih-Yang, and Rei-Tang Tsai. "Fluid mixing via multidirectional vortices in converging–diverging meandering microchannels with semi-elliptical side walls." *Chemical engineering journal* 217 (2013): 320-328.

[28] Alam, Afroz, and Kwang-Yong Kim. "Mixing performance of a planar micromixer with circular chambers and crossing constriction channels." *Sensors and Actuators B: Chemical* 176 (2013): 639-652.

[29] Yang, Jun, Li Qi, Yi Chen, and Huimin Ma. "Design and fabrication of a three dimensional spiral micromixer." *Chinese Journal of Chemistry* 31, no. 2 (2013): 209-214.

[30] Feng, Xiangsong, Yukun Ren, and Hongyuan Jiang. "An effective splitting-and-recombination micromixer with self-rotated contact surface for wide Reynolds number range applications." *Biomicrofluidics* 7, no. 5 (2013): 054121.

[31] Ansari, Mubashshir A., Kwang-Yong Kim, Khalid Anwar, and Sun Min Kim. "Vortex micro T-mixer with non-aligned inputs." *Chemical Engineering Journal* 181 (2012): 846-850.

[32] Scherr, Thomas, Christian Quitadamo, Preston Tesvich, Daniel Sang-Won Park, Terrence Tiersch, Daniel Hayes, Jin-Woo Choi, Krishnaswamy Nandakumar, and W. Todd Monroe. "A planar microfluidic mixer based on logarithmic spirals." *Journal of Micromechanics and Microengineering* 22, no. 5 (2012): 055019.

[33] Afzal, Arshad, and Kwang-Yong Kim. "Passive split and recombination micromixer with convergent–divergent walls." *Chemical Engineering Journal* 203 (2012): 182-192.

[34] Sheu, Tsung Sheng, Sin Jhih Chen, and Jyh Jian Chen. "Mixing of a split and recombine micromixer with tapered curved microchannels." *Chemical engineering science* 71 (2012): 321-332.

[35] Hossain, Shakhawat, Mubashshir A. Ansari, Afzal Husain, and Kwang-Yong Kim. "Analysis and optimization of a micromixer with a modified Tesla structure." *Chemical Engineering Journal* 158, no. 2 (2010): 305-314.

[36] Ansari, Mubashshir Ahmad, Kwang-Yong Kim, Khalid Anwar, and Sun Min Kim. "A novel passive micromixer based on unbalanced splits and collisions of fluid streams." *Journal of Micromechanics and Microengineering* 20, no. 5 (2010): 055007.

[37] Dreher, Simon, Norbert Kockmann, and Peter Woias. "Characterization of laminar transient flow regimes and mixing in T-shaped micromixers." *heat transfer engineering* 30, no. 1-2 (2009): 91-100.

[38] Ansari, Mubashshir Ahmad. "Parametric study on mixing of two fluids in a three-dimensional serpentine microchannel." *Chemical Engineering Journal* 146, no. 3 (2009): 439-448.

[39] Hossain, Shakhawat, M. A. Ansari, and Kwang-Yong Kim. "Evaluation of the mixing performance of three passive micromixers." *Chemical Engineering Journal* 150, no. 2-3 (2009): 492-501.

[40] Tofteberg, Terje, Maciej Skolimowski, Erik Andreassen, and Oliver Geschke. "A novel passive micromixer: lamination in a planar channel system." *Microfluidics and Nanofluidics* 8, no. 2 (2010): 209-215.

[41] Bhagat, Ali Asgar S., Erik TK Peterson, and Ian Papautsky. "A passive planar micromixer with obstructions for mixing at low Reynolds numbers." *Journal of micromechanics and microengineering* 17, no. 5 (2007): 1017.

[42] Wong, Seck Hoe, Michael CL Ward, and Christopher W. Wharton. "Micro T-mixer as a rapid mixing micromixer." *Sensors and Actuators B: Chemical* 100, no. 3 (2004): 359-379.

[43] Tsai, Tsung-Hsun, and Reiyu Chein. "Performance analysis of nanofluid-cooled microchannel heat sinks." *International Journal of Heat and Fluid Flow* 28, no. 5 (2007): 1013-1026.

[44] Lee, Jaeseon, and Issam Mudawar. "Assessment of the effectiveness of nanofluids for single-phase and two-phase heat transfer in micro-channels." *International Journal of Heat and Mass Transfer* 50, no. 3-4 (2007): 452-463.

[45] Chein, Reiyu, and Jason Chuang. "Experimental microchannel heat sink performance studies using nanofluids." *International journal of thermal sciences* 46, no. 1 (2007): 57-66.

[46] Hasan, Mushtaq I., Abdul Muhsin A. Rageb Rageb, and Mahmmod Yaghoubi. "Investigation of a counter flow microchannel heat exchanger performance with using nanofluid as a coolant." (2012).

[47] Dundi, T. Manoj, V. R. K. Raju, and V. P. Chandramohan. "Numerical evaluation of swirl effect on liquid mixing in a passive T-micromixer." *Australian Journal of Mechanical Engineering* (2019): 1-15.

[48] Jain, Mranal, Abhijit Rao, and K. Nandakumar. "Numerical study on shape optimization of groove micromixers." *Microfluidics and nanofluidics* 15, no. 5 (2013): 689-699.

[49] Engler, Michael, Norbert Kockmann, Thomas Kiefer, and Peter Woias. "Numerical and experimental investigations on liquid mixing in static micromixers." *Chemical Engineering Journal* 101, no. 1-3 (2004): 315-322.